SEMMELWEIS EGYETEM

DOKTORI ISKOLA

Ph.D. értekezések

3270.

LÉVAI ESZTER

Gyermekkori betegségek klinikuma, élettana és prevenciója

című program

Programvezető: Dr. Szabó J. Attila, egyetemi tanár

Témavezetők: Dr. Szabó J. Attila, egyetemi tanár és

Dr. Claus Peter Schmitt

PERITONEAL MEMBRANE SOLUTE TRANSPORTER EXPRESSION AND FUNCTION IN HEALTH, CHRONIC KIDNEY DISEASE AND PERITONEAL DIALYSIS

PhD thesis

Eszter Lévai, MD

Rácz Károly Conservative Medicine Division

Semmelweis University

Supervisors:

Prof. Attila J. Szabó MD, D.Sc, Prof. Claus P. Schmitt MD. DHC

Official reviewers: **Andrea Berkes MD, PhD, Ákos G. Pethő MD, PhD**

Head of the Complex Examination Committee: **András Szabó, MD, D.Sc.**

Members of the Complex Examination Committee: **Tamás Szabó, MD, PhD and András Tislér, MD, PhD**

Budapest

2025

Table of Contents

List of Abbreviations

AGE - advanced glycation end product

AlaGln – alanyl-glutamine

AQP-1 – aquaporin-1

BBB – blood-brain barrier

CAKUT – congenital

CKD – chronic kidney disease

CLDN - claudin

CPDF – conventional peritoneal dialysis fluid

CV - cardiovascular

(e)GFR - (estimated) glomerular filtration rate

EMT – epithelial-to-mesenchymal transition

ENaC -epithelial sodium channel

EPS – encapsulating peritoneal sclerosis

ESKD – end-stage kidney disease

FITC – fluorescein isothiocyanate

GLUT1/-2/-3 – glucose transporter – 1/-2/-3

GDP – glucose degradation product

HD - hemodialysis

HPMC - human peritoneal mesothelial cell

HUAEC - human umbilical arteriolar endothelial cell

HUVEC - human umbilical vein endothelial cell

IL-6/IL-17/IL-33 - interleukin-6/-17/-33

IQR - interquartile range

KDIGO - Kidney Disease Improving Global Outcomes

KRT - kidney replacement therapy

KTx - kidney transplantation

L/V ratio - lumen to vessel diameter ratio

LPDF - low glucose degradation product content peritoneal dialysis fluid

OCL - occludin

PC Transwell - polycarbonate Transwell

PD - peritoneal dialysis

PET - peritoneal equilibrium test

PiT1/SLC20A1 - sodium-dependent phosphate transporter protein-1

RT – room temperature

SD - standard deviation

SGLT1/-2 – sodium/glucose cotransporter-1/-2

SMLM - single-molecule localization microscopy

SONG PD - Standardized Outcomes in Nephrology-Peritoneal Dialysis

TER -transendothelial electrical resistance

TJ - tight junction

TriC - tricellulin

VEGF-A -vascular endothelial growth factor - A

ZO - zonula occludens

3,4-DGE - 3,4-dideoxyglucosone-3-ene

1 Introduction

1.1 Chronic kidney disease and kidney replacement therapies in childhood - the need for experimental research

Chronic kidney disease (CKD) is increasingly common worldwide, leads to major cardiovascular complications, a reduced life-expectancy and places a heavy burden on healthcare systems. Almost 850 million adult individuals are affected globally (1) and approximately 1.5 million grown-ups are involved in Hungary. (2) There is an estimated 2 million children affected by CKD stages 2-5 out of 2 billion children worldwide. This number is comparable to the predicted number of pediatric patients with type 1 diabetes and tenfold the number of children with cystic fibrosis. (3) This makes CKD one of the most common noncommunicable diseases. Despite the significance of this complex disease group with diverse etiology in children, awareness and public health effort for early diagnosis and prevention remain inferior to adult patient care and to other pediatric chronic diseases.

In end-stage kidney disease (ESKD) kidney transplantation (KTx) is the optimal kidney replacement therapy (KRT), having a superior survival rate compared to dialysis. Five-year survival rates are 80% with KTx vs. 53% on dialysis (4). However, KTx has limited availability due to the shortage of donor organs and various underlying diseases with associated comorbidities precluding KTx (5). With the steadily increasing number of CKD patients, the reliance on dialysis as a life-maintaining therapy is growing significantly. Peritoneal dialysis (PD) and hemodialysis (HD) are both suitable for bridging- and long-term therapies. There are controversial results regarding the superiority of one dialysis method over the other with respect to the hard outcomes such as mortality, suggesting a rather complimentary role and the need of individualized decision making. In pediatrics, PD is the preferred dialysis mode, since it provides a wide flexibility for school-aged children, less hospital visits and thus a better quality of life. PD does not require a permanent vascular access, which is particularly relevant in infants and young children and is more cost-effective in most countries (6).

This thesis focuses on the peritoneum as a dialysis membrane, the underlying molecular mechanisms of peritoneal solute transport and CKD and PD induced expression and functional alterations. As a proof of concept, a first experimental pharmacological

intervention reversing PD induced changes is presented. This is of particular interest in view of the increasing affected population and time spent on PD per individual.

1.1.1 Etiology and complications of CKD

CKD leads to a gradual, irreversible loss of kidney function over time. KDIGO defines it as abnormalities of kidney structure or function (glomerular filtration rate, GFR, in mL/min/1.73 m^2 body surface area), present for more than 3 months, with implications to health. (7) The rising numbers of CKD patients worldwide are mainly but not only due to adult patients, and originates from the increasing prevalence of hypertension, diabetes mellitus and obesity. While adult and pediatric CKD share the basic pathophysiological background, the leading causes of ESKD in children are different. Most common pediatric underlying diseases are congenital anomalies of the kidney and urinary tracts (CAKUT) (approx. 50%), steroid resistant nephrotic syndrome (approx. 10%), chronic glomerulonephritis (e.g. lupus nephritis, Alport syndrome, approx. 8%) and renal ciliopathies (approx. 5%) (8-11).

Etiology leading to CKD is age dependent with structural causes predominating in younger patients, while glomerulonephritis being the leading cause over the age of 12 years (9, 12). Premature, low-birth weight and small for gestational age newborns suffer from a reduced nephron number, predisposing to CKD. With the growing prevalence of childhood obesity and improved premature care, the future distribution of causes of CKD are destined to change, introducing new challenges to pediatric nephrologists. Pediatric CKD has additional peculiarities, such as highly dynamic mineral bone disorder and reduced growth, substantially contributing to exceedingly high cardiovascular diseases, which manifest already in childhood. (13) Children with kidney failure have a 30-60-fold higher mortality risk than the age-related healthy population. (14, 15)

1.1.2 Classification of CKD, ESKD

According to KDIGO 2024 Clinical Practice Guideline for the Evaluation and Management of Chronic Kidney Disease six categories of CKD are distinguished according to GFR categories (G1, G2, G3a, G3b, G4, G5) (14). This dissertation is focused on CKD G5 (CKD5), also called end stage kidney disease (ESKD) requiring dialysis or the stage CKD5, i.e. individuals actual on dialysis.

According to pediatric guidelines, PD should be initiated, when the creatinine clearance is < 10 ml/min/1.73 m^2 and/or when there are symptoms and signs of uremia and/or growth failure (15). At this stage (CKD5), mild changes in the peritoneal ultrastructure and cellular profile have developed.

1.2 Peritoneal morphology and function

1.2.1 Peritoneal membrane structure

The peritoneum is a thin serosal membrane that lines the abdominal cavity and internal organs. The peritoneal surface area is proportional to the body surface area (16). The peritoneum is divided into the parietal peritoneum lining the abdominal wall and the pelvic cavity, and the visceral peritoneum covering the outer surface of abdominal organs.

Multiple functions of the peritoneal membrane are crucial to the local and systemic homeostasis, such regulating inflammatory, fibrotic and angiogenetic processes, exchanging abdominal fluids, providing nutrition and mechanical support to the abdominal organs, and protection from frictions and adhesions. (17) Being involved in internal organ development, with biochemical signals driving and sustaining cell transition (18, 19) and also regulating pathophysiological processes regarding tumor progression in the peritoneum, and post-infectious and postinterventional adhesions, make it an organ of high importance. (20)

Schaefer et al has first described the healthy peritoneal ultrastructure in detail. (21)

The mesothelial cell layer, a cell monolayer at the surface of the mesothelium showed calretinin and E-cadherin positivity and was also positive in immunohistochemistry studies for AQP-1, suggesting a role in transport.

Mesothelial cells have a prominent role in the induction of fibrosis, by formation of cell protrusions, adjoining the opposing mesothelial surfaces, when exposed to sustained noxious stimuli. (22-24) Protrusion forming is also an important mechanism in malignant mesothelial cell metastases. (25) Both functions require rearrangement in mesothelial cell-to-cell communication involving proteins of the paracellular pathways, the tight junctions. (26, 27)

Its utmost functional importance in PD transport, in opposition with former theories has been proven by a recently published paper by our group (Marinovic et al.) which is not discussed in detail in this dissertation. (28) The mesothelial coverage is unchanged during CKD and the first two years of PD, but a progressive loss has been shown thereafter. (28)

The submesothelium, composed of extracellular matrix, small blood vessels and fewer lymphatic vessels and nerves. (21) Submesothelial thickness was increasing after infancy and was lower again in adulthood. Total peritoneal microvessel density was also age-dependent, forming a U-shaped curve starting from infancy. Importantly the capillary endothelial surface area per volume of peritoneal membrane and likewise, lymphatic endothelial surface area per volume of peritoneal membrane was threefold higher in the first year of life. The endothelium of blood capillaries and lymphatic vessels were built up by a single endothelial cell layer. No vasculopathy, epithelial-to-mesenchymal transition (EMT) or calcification was present in healthy children. (21)

The ultrastructural changes of the peritoneal membrane already start at CKD, and accelerate amid the supraphysiological glucose-, GDP- and uremic toxin concentrations of PD. During peritoneal dialysis peritoneal inflammation and progressive fibrosis are present. Reorganization of the peritoneal membrane can differ regarding the glucose degradation product (GDP) content of the PD fluid. Low GDP PD treatment can promote early angiogenesis, while high GDP PD triggers apoptosis and development of vasculopathy. (29) Increased vascularization impacts small solute transport. (29) Elevated lymphatic vascularization affects the escalation of peritoneal absorption. (30) Progressive fibrosis in the submesothelium and vasculopathy defines a reduced osmotic conductance of glucose and therefore reduces the fluid removal capacity. (31)

Studies on the molecular counterparts of solute transport, i.e. purification function of PD are lacking.

1.2.2 The peritoneum as a dialysis membrane, the 3-pore model

The peritoneum works as an endogenous semipermeable dialysis membrane and is being used as a peritoneal dialyser for more than 50 years. The primary goal is the removal of excessive water and small solutes (e.g. creatinine) and middle-size molecules (e.g. ß-2 microglobulin) in ESKD. However, there are major limitations of PD, namely a limited efficacy of purification and a limited sustainability of PD. The PD membrane is

progressively transformed with time on PD, and effectivity of toxin-, salt- and water removal declines. (29, 32)

In 1993, Rippe and his colleagues described peritoneal transport with a mathematical model, only considering the endothelium as a key barrier for transport. [Figure 1.] The „3-pore model" hypothesizes three different sizes of pores for the exchange of molecules, a) transcellular/ultrasmall pore, primarily responsible for water transport (aquaporin-1 - AQP1), b) small pore, responsible for small solute and ion transport, and c) the large pore, subject of macromolecule transport. Only the molecular counterparts of the transcellular pore, AQP-1 is identified to date. (33) In mice with global AQP-1 knock-out peritoneal water transport is 50% reduced (34-36) In clinical setting, promoter variants of AQP1 also influence ultrafiltration and are associated with technique failure and mortality rates in patients on chronic PD. (37) The molecular mechanisms of the remaining water and of solute removal is still uncertain.

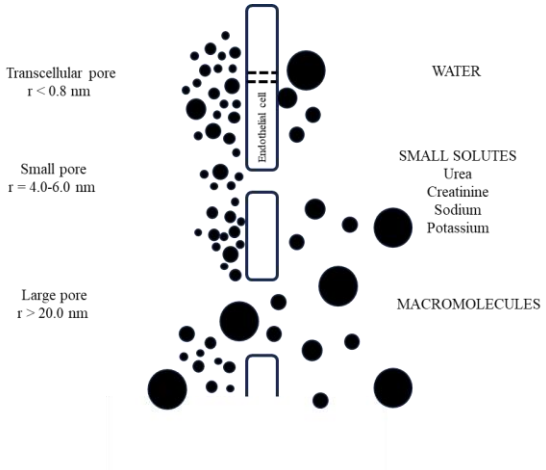

Figure 1. A simplified diagram of the peritoneal, size-selective transport described by the 3 pore model based on Flessner et al. (38)

1.3 Complications of peritoneal dialysis

1.3.1 Infectious complications

The most common complication of PD is peritonitis. The acute, and in many cases repeated infections contribute to the reorganization of the membrane, and often the revision of the catheter or discontinuation of PD. Catheter exit-site infections are also infectious complications, potentially leading to secondary infection of the abdominal cavity.

1.3.2 Changes of the peritoneal membrane structure and transporter status, ultrafiltration failure

During PD, the peritoneal membrane undergoes major transformation. (29) As mentioned, these alterations begin already prior to dialysis, during CKD, where mild chronic parietal peritoneal inflammation is already present, just as epithelial-to-mesenchymal transition and vasculopathy.

So called conventional PD fluids are high in glucose degradation products (GDPs), lactate and have an acidic pH. They induce peritoneal submesothelial fibrosis, progressive peritoneal mesothelial cell loss and vasculopathy. (29) Two chamber PD fluids have a substantially reduced GDP-content and a neutral to physiological pH and contain either lactate or bicarbonate as buffer compound. These fluids have been classified as biocompatible fluids, however, they also cause early peritoneal inflammation, fibroblast activation and EMT, together with a marked angiogenesis, that correlates with the PD membrane transport function. (39) Fluids with novel osmolytes, such as icodextrin, have been introduced two decades ago, and improve patient outcome due to reduced dialytic glucose exposure and associated sequelae. (40, 41)

Peritoneal solute transport function is classified into low, low-average, high-average and high transporters, based on the peritoneal equilibrium test (PET). (42) [Figure 2] PET tests are advised to be done both before the dialysis start, and then once yearly or in case of clinical complications to monitor the changes in the transporter status and adjust the dialysis regime accordingly. The PET quantifies the movement of small solutes urea, creatinine and glucose, based on sampling of serum and dialysate effluent at different time points (0.-120/240 min). Faster transporters exchange solutes faster, i.e. have a higher solute clearance capacity but also have a faster glucose uptake, and lose the osmotic gradient required for ultrafiltration. During the course of long-term PD, patients develop a faster transporter status and eventually lose the capability of adequate ultrafiltration. (43, 44)

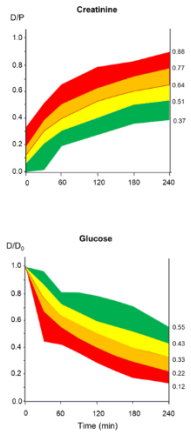

Patients (%)	Type	4-hours D/P creatinine	Characteristics
10%	High	> 0.78	Rapid solute transport Absorption of glucose: Reduced UF Loss of proteins? Serum albumin?
53%	High Average	0.65 - 0.77	Good solute transport Sufficient UF
31%	Low Average	0.52 - 0.64	Solute transport relatively slow Good UF
6%	Low	< 0.51	Slow solute transport Clearance targets difficult to achieve Very good UF

Figure 2. Peritoneal transporter status according to the results of the peritoneal equilibrium test (PET). The Dialysate(Crea)/Plasma(Crea) (D/P_{Crea}) and the D/D_0 ratio for glucose ratios categorize patients in four groups of peritoneal transport function. On the graphs the five lines dividing the four areas (four categories of transporters) are the maximum value. (Modified from Warady BW et al, 1996) (45)

As an additional complication, peritoneal protein leakage can increase with chronic PD due to an insufficient cellular barrier function. Increasing peritoneal protein loss predicts worse outcome regarding cardiovascular events, peritonitis and also death, while the link with technique survival is unclear. (46-50)

1.4 Transport components of the peritoneal membrane – paracellular and transcellular proteins

Peritoneal permeability is characterized by transcellular and paracellular transport. Considering the peritoneum as a leaky membrane, allowing for rapid diffusion of water and small solutes, paracellular pathways have a major role in underlying transport mechanisms. (51-53) Tight junctions (TJ) are the key elements of mostly permselective paracellular transport in endothelial and epithelial barriers, and also indirectly effect transcellular transport properties. They ensure the polarization of these monolayers and their proper operation as barriers. Many physiological functions rely on this barrier role to sustain physiological cell and organ function (54). Proper function of TJ proteins is crucial for preserving the physiological permeability of the endothelial barrier. (55) Previously it was assumed, that the mesothelial cell layer has limited barrier function,

compared to the endothelium, based on mathematical modelling (56) and comparison of the electrophysiological monolayer characteristics of endothelial and mesothelial cells (57). In this dissertation the paracellular properties of both the mesothelial and endothelial compartment is described in depth.

Paracellular permeability has not yet been described before in detail regarding the peritoneum, of other cellular membranes is controlled by claudins and the TJ-associated MARVEL proteins occludin (OCL), tricellulin (TriC) and marvelD3. Currently there are 27 described members of the claudin (CLDN) family, in the work of this dissertation the following molecules were chosen to be discussed in detail: the pore-forming claudin 2, -4, -15, facilitating the paracellular transport of water and sodium (CLDN2 and CLDN15) and chloride (CLDN4), and on the sealing group of claudin 1, -3, -5, responsible for reducing the paracellular conductance. (58)

CLDN2, -4, and -15 are pore-forming claudins. Claudin-2 is a paracellular channel for small cations and water, both transports occurs through the same pore. (59, 60) Increased expression of CLDN2 leads to impaired barrier function. (61) CLDN4 plays a major role in the intestines and exerts chloride transport. (62) CLDN4 is a receptor of the Clostridium perfringens toxin. It is not expressed in Williams-Beuren syndrome, the specific functional consequences are not yet clarified. CLDN4 probably covers a wide range of functions, many yet unknown. (63, 64) CLDN15 is also a paracellular channel for small cations and water, but with a distinct function to CLDN2. (65)

The sealing group of claudins, (e.g.CLDN1, -3, -5) reduce paracellular conductance. (58) CLDN1 is a paracellular barrier molecule against transepithelial diffusion, defining epithelia as tight, with almost impermeable tight junctions, such as the human epidermis. (66-68) It also plays a role in oncological diseases, such as hereditary mammary cancer, colorectal, ovarian or pancreatic cancer. (69) CLDN3 is a general barrier forming molecule, also typical for tight epithelia, with no charge preference for ions, and like CLDN4 a receptor for Clostridium perfringens enterotoxin. (62, 70) CLDN3 also forms complexes with various other proteins of the claudin family. (71, 72) CLDN5 is considered to be the most important TJ component protein for endothelia, mediating cell-cell interactions (73). Its presence and function has also been confirmed in epithelial barriers, e.g. in intestinal barrier (74) CLDN5 is deleted in the velo-cardio-facial

syndrome (DiGeorge syndrome), and CLDN5-deficient mice exhibit blood-brain-barrier defect. (75, 76)

The zonula occludens family consists of 3 members: ZO-1-3. Zonula occludens-1 (ZO-1) is a significant scaffolding protein bridging TJ claudins to the actin cytoskeleton. (77, 78) Occludin function is only partially understood. In OCL knock-out mice it regulates paracellular permeability under hydrostatic pressure shifts but does not alter intestinal barrier function by default. Tricellulin is a TJ protein present at the meeting surface of three cells, regulating the passage of macromolecules (79, 80).

With the abovementioned transporters as the focus of my studies it is possible to get a valid understanding of epithelial and endothelial paracellular sealing functions (CLDN1, CLDN5) in the peritoneum. It is also feasible to study small cation and anion transport, and water transport with focusing on CLDN2, CLDN3, CLDN4 and CLDN15, getting a broader picture on possible small molecule transport.

Scaffolding and structural TJ proteins (ZO-1, OCL) were chosen to understand the overall function of the TJ complex.

The transcellular pathways consist of water and ion channels of the plasma membrane, such as the abovementioned AQP-1 and the epithelial sodium channel (ENaC), the sodium-glucose co-transporters-1 (SGLT1) and sodium/phosphate cotransporter PiT1/SLC20A1 (PiT1) studied in this dissertation. The distribution of sodium-glucose co-transporters-2 (SGLT2) in the peritoneum, intensively discussed in other fields of nephrology, in addition to glucose transporter-1 and -3 (GLUT-1, -3) has already been described, showing regular expression of these transporters in PD patients and the increased expression of SGLT-2 with PD duration and a significant enhancement of this molecule in encapsulating peritoneal sclerosis (EPS) patients. (81) SGLT-2 inhibition in mice has significantly reduced peritoneal fibrosis and microvessel density, thus improved ultrafiltration, although did not influence the development of high-glucose transporter status. (82) These results pinpoint the importance and possibilities still hidden in studies addressing peritoneal transport proteins.

Detached mesothelial cells isolated from patients' dialysate effluent also express various TJ proteins (CLDN1, -2-, -8, OCL, ZO-1) in altered levels compared to non-dialysed controls and decreased expression in high- versus low transporters. (83) TJ proteins quantified in the PD effluent, originating from detached mesothelial cell, may also have

a connection with the PD fluid induced insult to the mesothelium. (84) Glucose, oxidative stress and proinflammatory cytokines can cause expressional changes in TJ components and ultrastructural reorganization of the TJ. In vitro, glucose and reactive oxygen species reduce ZO-1, OCL and CLDN1 expression in human primary peritoneal mesothelial cells (HPMC), but not the glucose polymer used in new generational PD fluids, icodextrin (40, 41).

Altogether these findings illustrate the importance of the paracellular and transcellular pathways, and the lack of knowledge regarding peritoneal transport, the significant lack of knowledge regarding, and by this the lack of knowledge on potential therapeutic interventions to enhance PD efficacy.

1.4.1 Vascular disease alterations in CKD and during PD

Due to a plethora of pathomechanisms accumulating with CKD and additional factors such as the enhanced dialytic glucose exposure during PD, PD patients suffer form an exceedingly, 40-times increased cardiovascular risk relative to the age-matched general population (85). In 2020 the Standardized Outcomes in Nephrology-Peritoneal Dialysis (SONG-PD) initiative established a core outcome set for future trials, based on the shared priorities of patients, caregivers and health professionals. Cardiovascular complications were one of core outcomes according to all stakeholders. (94) This underlines the essential need of further research. In this context peritoneal and omental vascular tissues provide a unique scientific window, especially when these tissues are collected from children. Children are virtually devoid of any aging and lifestyle related factors, such as smoking or alcohol consumption, and the underlying diseases in the majority of cases do not affect the systemic vascular integrity, as in most cases they are limited to the kidney and urinary tract. Key driving factors of local systemic damage associated with PD fluid administration are supraphysiological concentrations of glucose in dialysis fluids and in conventional PD fluids also the high amounts of GDPs, generated during the heat sterilization process and during prolonged storage. GDPs are rapidly absorbed into the circulation, increasing the systemic advanced glycation end product (AGE) concentrations. (86-88) Additional local damage is exerted by conventional PD fluids due to the acidic pH. Different from adults, children on PD rarely develop diabetes mellitus, blood glucose concentrations remain the physiological range. (89) This, however, does not preclude major vascular consequences. A recent transcriptome-proteome cross-omics

study in arterioles demonstrated major complement activation in PD patients associated with vascular disease (90). Comprehensive data on the molecular pathomechanisms induced by the GDP load on cardiovascular health is largely unknown. This dissertation used omental arterioles to assess systemic vasculopathy, as surrounded by fat tissue, they are protected from immediate PD-fluid induced effects, and they also represent key segments of the vasculature defining blood pressure (91). The analysis was focused on vascular transporter molecules such as ZO-1 also involved in inflammation, apoptosis and early vasculopathy (92-95) and CLDN5, the primary sealing claudin in endothelium.

1.4.2 Preserving the peritoneal membrane function

CKD and PD patients suffer from long standing complications of uremia and KRT. Underlying mechanisms still remain only partially understood. PD has been administered as a successful KRT for more than 60 years, and yet the basic principles of therapy remained largely unchanged. The superiority of a newer generation of biocompatible fluids is still a divisive topic, and even these fluids have a transformative effect on the peritoneal membrane (96-101). However, with the increasing number of ESKD patients, the need for long-term, effective PD therapy is growing. Fluids with novel osmolytes, such as icodextrin, have been used in the past two decades and since no new products have been introduced for wider usage in the PD fluid market. In the same direction, PD fluids with protective additives counteracting local and systemic pathomechanisms should result in improved PD technique and patient outcome (102, 103). Enhancing PD treatment efficacy is essential for improved patient outcomes, and in-depth exploration of the still largely unknown underlying mechanisms of transport and membrane transformation is essential.

2 Objectives

During the time of my PhD studies, the aim was to investigate yet little described components of peritoneal membrane transport, i.e. tight junction molecules, transporters and channels during the course of CKD and PD treatment. The following questions have been addressed.

1. Expression of key molecules of peritoneal trans-and paracellular transport in health, CKD and during PD in mesothelium and endothelium in the peritoneal membrane
2. Correlation of peritoneal transcellular and paracellular protein expression and peritoneal membrane function during PD
3. Establishment of an experimental workflow for studying barrier integrity and permeability within the same polarized cell monolayer of interest in the context of PD, mesothelial and endothelial mono-cell layer barriers.
4. Reversing the PD-fluid induced disintegration of the endothelial membrane by pharmacological means (with AlaGln)
5. The effect of high GDP load in PD on endothelial cell junction and cytoskeleton disruption in vasculopathy

3 Methods

3.1 Patient selection and sampling of the international peritoneal biobank

All immunohistochemistry studies listed in this dissertation were performed according to the following principles: “[p]eritoneal tissues were collected within the International Peritoneal Biobank (IPPB, registered at www.clinicaltrials.gov—NCT01893710) as described previously. (21) The study was performed according to the Declaration of Helsinki which sets ethical principles regarding human experimentation. The Ethical Committee of the Medical Faculty at the University of Heidelberg and institutional boards from all participating centers approved the study protocol and consent forms. Written informed consent was obtained from the patient’s parents and patients as appropriate.” (104).

In the experiments performed in transporter studies, we have investigated “46 individuals with normal renal function for analysis of age-related junction and transcellular transporter abundance were analyzed (age 0–75 years), 23 children with CKD5 and 24 children on PD for 12.8 (IQR 7.9, 21.9) months with neutral pH PD fluids with low glucose degradation product content. Individuals with a body mass index (BMI) of > 35 kg/m2 and with chronic inflammatory diseases, and diseases affecting the peritoneum were excluded. Tissues in individuals with normal renal function were collected during abdominal surgeries unrelated to kidney and during living donor kidney transplantation. Tissues from children with CKD5 were obtained at the time of PD catheter insertion, in PD patients at the time of catheter revision and/or exchange, kidney transplantation, hernia/leakage” (104) all other details (the length of PD, exact dialytic glucose exposure and peritonitis episodes, treated successfully) are discussed in the relating publication. (104)

Parameters of children with normal kidney function, patients with CKD5 and patients on PD were compared matched for age and body surface are (BSA).” Biochemical characteristics are described in the related article. ”In 23 patients (21 on cycling PD), peritoneal equilibration test (PET) was performed to assess peritoneal transport function. PET was performed according to standard guidelines and 2 h D/P creatinine and D/D0 glucose were measured (105-107). The underlying diseases of these 23 patients and their biochemical findings did not differ from the rest of the group.”

In the study about glucose derivative induced vasculopathy the main principles of patient selection criteria were the same as the abovementioned, with the following certain differences. “After matching for age, glucose exposure, and PD duration, parietal peritoneal tissue of 60 double-chamber, low-GDP and 30 single chamber, high-GDP PD fluid–treated patients were selected and age-matched to 107 children with CKD5. Individual GDP exposure was calculated from the actual PD regime and GDP content of the administered PD, as published previously (108, 109).“ (110) The molecular background of vasculopathy was studied in microdissected omental arterioles in CKD5, low-GDP PD and high GDP PD patients. For transcriptome and proteome analysis mRNA and protein were isolated (n=8 in CKD5, n=6 for high-GDP, and n=5 for low-GDP group), not discussed in further detail here. ”For validation of the key molecular pathways identified by cross-omics in arterioles, parietal peritoneal tissue of 10 patients with low- and high-GDP PD … underwent digital immunohistochemistry analyses.” (110)

3.2 Histological studies

Immunohistochemical stainings were performed on formalin-fixed tissue sections according to standard methods and all markers were stained as described previously. (29) (35) The following antibodies were used: ASMA (Dako Cytomation, Denmark, 1:1000), calretinin (Cell Marque, CA, USA, 1:100), CD31 (1:25), CD45 and CD68 (both 1:100), podoplanin (1:1000) were from Dako Cytomation, Denmark. Claudin-1–5, OCL, TRiC and ENaC were from Thermo Fisher Scientific, MA, USA (all 1:500), ZO-1 (LifeSpan Biosciences, USA, 1:500), SGLT1 (Millipore, USA, 1:2000), PiT1 (SLC20A1) (Thermo Fisher Scientific, MA, USA, 1:500). Secondary antibodies (against the host species of the first antibody were purchased from Thermo Fisher Scientific, MA, USA, 1:300). Immunofluorescence stainings were performed according to standard methods. After dewaxing, heat induced antigen retrieval was performed in microwave. Claudin-5 conjugated with Alexa 488, ZO-1 conjugated with Alexa 555 (Thermo Fisher Scientific, MA, USA, 1:1000) and claudin-2 primary antibody was applied overnight and after washing, secondary Alexa 647 (Thermo Fisher Scientific, MA, USA, 1:1000) antibody added. Cell nuclei were counterstained with DAPI (Thermo Fischer, MA, USA, 1:1000).

3.3 Digital image analysis

"Submesothelial thickness was measured at least 5 different sites of CD31 stained scanned sections. Microvessel density was analyzed from CD31 stained tissues and was defined as the number of vessels per unit of analysis area. Podoplanin and CD31 positive vessels were defined as lymphatics. Blood vessel density was calculated from the density of CD31 stained capillaries minus podoplanin positive lymphatics. Diffuse podoplanin staining phenotype was defined as extra-lymphatic (podoplanin positive, but CD31 negative) podoplanin abundance as previously described (29)." (104) Capillary vessel area was defined as:

$$\frac{\text{endothelial area} + \text{lumen area and capillary wall}}{\text{intimal thickness}}$$

The capillary endothelial surface area relative to peritoneal volume was calculated by:

$$\frac{\text{endoluminal perimeter of CD31 stained endothelium} \times \text{section thickness} \times \text{number of vessels}}{\text{analyzed peritoneal area} \times \text{section thickness}} \left(\frac{\mu m2}{\mu m3}\right)$$

"CD45 positive leukocytes, CD68 positive macrophages and ASMA positive cells were quantified per mm2 of submesothelial area. Semi-quantitative score was applied for mesothelial coverage (0–6, with 0 = no or isolated cells present only, and 6 representing complete coverage). Mesothelial cells identified as calretinin positive cells in the submesothelium with phenotypic signs of fibroblasts were defined as EMT cells and quantified per mm2 sub mesothelium. Arteriolar luminal diameter to vessel external diameter (L/V) was quantified on arterioles with a 60–100 μm diameter, average of L/V of 5 to 7 vessels per sample measured was taken as the representative value14. Digital image analyses Whole tissues slides were scanned and evaluated using the Aperio® Precision Image Analysis Software as described previously (29, 110). For quantification of junction and transcellular transporting proteins, positive Pixel Count Algorithm (Aperio® Technologies, Inc., Vista, California, USA version 9) was used and regions of interest (ROI) were annotated, excluding surrounding fat tissue and lumen. Intensity ranges were validated for each specific staining, and a threshold set for defining pixel positivity. Protein abundance was calculated as the number of positive pixels divided by total number of pixels, the latter being defined by the ROI area. Tissues for one marker were stained in one run, in case when more than one run was necessary, internal controls were used to normalize staining intensities to account for inter-staining variation. No

inflammatory cells were present in the mesothelial cell layer and only arterioles without inflammatory cell infiltration were analyzed. Confocal microscopy imaging z-stacks of DAPI, Alexa-488, Alexa-555 and Alexa-647 were acquired at × 400 magnification with Leica TCS SP5 (Leica Biosystems, Wetzlar, Germany) confocal microscope. Subsequent co localization and z-projection with maximal intensity were prepared using open-source FIJI software." (104)

Further details of automated imaging with ACQUIFER Imaging Machine, a widefield high-content screening microscope (ACQUIFER Imaging GmbH, Heidelberg, Germany), are listed in the corresponding publications. (55, 111)

3.4 Cell culture experiments

"Human umbilical vein endothelial cells (HUVEC) were commercially purchased (PromoCell, Heidelberg, Germany) and kept in endothelial cell growth medium with supplement and antibiotics (PromoCell, Heidelberg, Germany) in an incubator at 37 C and 5% CO2. All experiments were performed on cells within the first 5 passages." (111)

In our AlaGln supplementation experiments "[t]he HUVEC were incubated with acidic, (pH 5.5), lactate buffered PD fluid (CPDF; CAPD StaySafe ®, 2.3% glucose, Fresenius Medical Care, Bad Homburg, Germany), with high glucose degradation product content and with neutral pH, low glucose degradation product content, lactate buffered PD fluid (LPDF; Balance ®, 2.3% glucose, Fresenius Medical Care, Bad Homburg, Germany), and culture medium as control. Unspecific cytotoxicity was ruled out by lactate dehydrogenase (LDH) measurements in the supernatant photometrically in central laboratory (Analysezentrum, Heidelberg University Hospital, Heidelberg, Germany). Glucose concentration and calcium content (1.75 mmol/L) were the same in both PD fluids. An alanyl-glutamine dose-response curve was established, for further experiments, pharmacological dose of 8 mM was used, as established previously. (112)" (55)

3.5 Cell cultures, transendothelial electrical resistance and dextrane transport measurements

To measure transendothelial resistance during the establishment of the new experimental workflow for investigating monolayers, we have started with an in vitro model of human umbilical vein endothelial cells (HUVEC). For this monolayer "a cell suspension (5x10^4

cells/cm^2) was seeded and cultured on a polyester/polycarbonate mesh (Transwell, 0.4 m pore size, 12-well type; Costar, MA, USA) using standard culture conditions. The apical and basolateral chambers of the Transwell were filled with 0.2 mL and 1 mL culture medium, respectively." (111) We have used the same set-up in the AlaGln experiments too, with other fluids to incubate in. For these experiments, "[t]he HUVEC were incubated with acidic, (pH 5.5), lactate buffered PD fluid (CPDF; CAPD StaySafe ®, 2.3% glucose, Fresenius Medical Care, Bad Homburg, Germany), with high glucose degradation product content and with neutral pH, low glucose degradation product content, lactate buffered PD fluid (LPDF; Balance ®, 2.3% glucose, Fresenius Medical Care, Bad Homburg, Germany), and culture medium as control. Unspecific cytotoxicity was ruled out by lactate dehydrogenase (LDH) measurements in the supernatant photometrically in central laboratory (Analysezentrum, Heidelberg University Hospital, Heidelberg, Germany). Glucose concentration and calcium content (1.75 mmol/L) were the same in both PD fluids. An alanyl-glutamine dose-response curve was established, for further experiments, pharmacological dose of 8 mM was used, as established previously (112)." (55)

"Transendothelial electrical resistance (TER) was measured daily using an EVOM volt ohm meter equipped with STX-2 electrodes (World Precision Instruments, Sarasota, FL, USA). The electrodes were inserted into both ends of the mesh. An alternating current of less than ±20 μA was applied between the electrodes at a frequency of 12.5 Hz. To calculate the normalized TER of each monolayer, the background TER of a blank filter was subtracted from the TER of the respective cell monolayer. The resistance of each monolayer was multiplied by the effective surface area (0.33 cm^2) corresponding to the filter size in order to obtain the electrical resistance of that monolayer (in Ω*cm^2). The treatment was initiated when each monolayer was fully formed as demonstrated by a plateau in the TER (4–6 days post-seeding), and the baseline TER was >10 Ω*cm^2. The data are presented as % fold change of the cells cultured in standard culture conditions (control)." (111)

To assess the paracellular endtothelial barrier dextrane transport in vitro, we measured the flux of 4 kDa, 10 kDa and 70 kDa fluorescently labeled dextrane with the same method. As an example the "flux of 10 kDa fluorescein isothiocyanate (FITC) labelled dextran (obtained from Sigma Aldrich, Taufkirchen, Germany) from the apical to the

basolateral compartment of a Transwell chamber as a function of time. More specifically, 1 mg/mL was added in the apical compartment of a Transwell chamber and the increase of the fluorescence intensity in the basolateral Transwell compartment after 4 h. An equimolar amount of unlabeled dextran was added to the basolateral compartment of the [T]ranswell system to maintain an isotonic condition. At 4 h after the addition of the 10 kDa FITC-dextran, a 10 µL volume of each sample was collected from both sides of the chamber. Each sample was assessed using a fluorescence spectrophotometer (F-2000; Hitachi, Tokyo, Japan) at an excitation wavelength of 490 nm and an emission wavelength of 520 nm. A calibration curve was established and used for the calculation of the amount of FITC dextran, which was transported to the lower compartment. Results are presented as % fold change of the cells cultured in standard culture conditions (control)." (111)

3.6 Immunostaining

To carry out immunostaining in the course of setting up the new experimental workflow and to implement it on AlaGln experiments, "[c]overglasses/filters were fixed in absolute ethanol at 20C for 5 min, washed, permeabilized (0.5% Triton X in PBS for 10 min), washed again and blocked (5% bovine serum albumin in PBS) for 1 h at room temperature (RT). Incubation with the primary antibody was performed overnight at 4C. The appropriate secondary fluorescent antibody was added on the next day for overnight at 4 C. For double-staining, coverglasses/filters were fixed again with 4% PFA for 20 min at RT, washed and incubated again with the primary antibody. Polyclonal antibodies were incubated first. Nuclei were stained with DAPI (1:1000). After washing, the filters were cut out from the plastic by a needle tip, put on glass slide, covered with Prolong Gold (Thermo Fischer Scientific, Dreieich, Germany) and let harden at least for 24 h at RT in the dark and kept at 4 C until analysis. PBS (1.25 mM Ca^{++} and 1.75 mM Mg^{++} was used to stabilize the cell membranes throughout the staining procedure." (111)

3.7 Western Blot

"Cells were lysed with whole cell lysis buffer (10 mM Tris, 150 mM NaCl, 0.5% TritonX-100, 0.1% SDS, protease inhibitor). Equal amounts of 30 g of total protein of each cell lysate were diluted with 4 loading buffer (containing 4%-mercaptoethanol). Proteins,

dependent on their expected size, were separated in a 10% or 12% polyacrylamide gel at 200 V for 45 min. The transfer of the protein onto a polyvinylidenfluoride membrane was performed in a Transblot Cell (Bio-Rad Laboratories, Munich, Germany) at 105 V for 90 min. The membrane was blocked with blocking buffer (3% bovine serum albumin, 5% milk) for 1 h at room temperature followed by incubation with specific antibodies against ZO-1 (LS-B5625, Life Span Biosciences, 1: 500) and CLDN5 (clone 4C3C2, ThermoFischer Scientific, 1: 500) overnight at 4 C on a shaker. The membrane was rinsed once and washed three times for 5, 10 and 15 min with 0.05% Tris-buffered saline with Tween 20 (TBS-T), then incubated for 1 hat room temperature with the secondary antibody (anti rabbit horseradish peroxidase conjugated, 1:3000). Following three further washing steps with 0.05% TBS-T, enhanced chemiluminescent signal detection was performed. Equal loading of protein was assessed by re-probing the membrane for glyceraldehyde 3-phosphate dehydrogenase (GAPDH, H86504M, Meridian Life Science 1: 20,000) for 30 min. The signals were scanned and quantified densitometrically using Image Lab Software ® (Bio-Rad, Hercules, CA, USA). “

Further details of the used murine model from the discussed article about AlaGln are published (55).

3.8 Single Molecule Localization Microscopy (SMLM) and data analysis

“For the SMLM experiments, a custom-made apparatus based on an iMic microscope (Till Photonics, FEI) was used (113-115). The SMLM system is equipped with an Acousto Optical-Tunable-Filter (AOTF), a variable beam expander (Standa Ltd., Vilnius, Lithuania), a Flat-Top-Profile forming optics—PiShaper (AdlOptica GmbH, Berlin, Germany), a 100x /NA1.46 oil plan apochromatic objective lens (Carl Zeiss Microscopy, Göttingen, Germany) and four lasers: 405, 491, 561, and 642 nm with maximal laser power of 120, 200, 200, and 140 mW, respectively. … The system was maintained free from environmental influences by thermomechanical stabilization ($\pm 10^{-2}$ K), constant monitoring of the temperature in the measurement environment and liquid cooling of the main critical components. The SMLM measurements were initiated after allowing an hour for thermal equilibrium used in order to avoid thermal expansion effects. The fluorescent light was recorded by an iXon Andor Ultra EMCCD camera (Andor Technology, Belfast, Northern Ireland) (80 nm/px, EM-gain set to 100). To allow for

comparisons among measurements, the following automatized image acquisition protocol was employed: After a 10 s and 20 s flash at 150 mW and 140 mW, respectively, fluorophores were set into a reversible bleached state. Subsequently, 2000 images (100 ms integration time) were recorded and stored as a 16-bit grey-scale *tiff image stack. In addition to the SMLM data stack, a widefield image of the relevant specimen region was recorded.

SMLM data analysis was performed with an in-house developed python-based package and the use of MATLAB software (116, 117). Following visual inspection, masks were interactively determined to limit analyses to membrane areas of neighboring cells. The programs detect the position of the blinking dye molecules, use a 2D Gaussian to calculate their position, and compile a matrix containing the signal amplitude, the x- and y-coordinates, and the corresponding errors. Based on this matrix, relative pairwise distance distribution histograms (0–200 nm) for Ripley's structuring analysis (117), signal counts, and pointillistic images of the CLDN5 and ZO-1 stained junction areas between two endothelial cells were created." (111)

3.9 Statistics

Descriptive data were summarized using proportions, means (SD), or medians (interquartile range)."(110) "AlaGln effect is shown as a percentage of the corresponding treatment group without AlaGln supplementation."(55) "Normal distribution was assessed graphically and by Shapiro-Wilk test, Pearson, or Spearman correlations were calculated as appropriate. T test or Mann-Whitney test were applied for testing of differences between 2 groups based on the data distribution. For describing differences in proportions, $\chi 2$ or Fischer exact test were used. Two-sided tests were applied unless stated otherwise. One-sided tests were used only in the validation cohort" of the arteriole studies "(n=10 per group) to confirm direction of regulation from comparison of 30 versus 60 patients for submesothelial thickness, microvessel density, blood vessel density, and lumen/vessel (L/V) ratio, which were significantly regulated."(110) In the presented studies, "[e]xperiments were performed at least 4 times in at least 3 replicates. (111) Based on the data distribution, associations between functional data and transport protein abudances were studied by Pearson and Spearman correlation analysis. Arteriolar CLDN2 abundance association with age and microvessel density was tested with

multivariable linear regression models. “One-way parametric ANOVA as well as nonparametric Kruskal-Wallis was implemented for multiple group comparisons, with Holm-Sidak and Dunn methods, respectively, to adjust for multiplicity.”(110) Details of immunofluorescent image statistical analyses and SMLM microscopy statistical analyses can be found in the corresponding two publications discussed in this dissertation. “For single-molecule localization microscopy cluster analysis and for ionic and solute permeability measurement, 2-way ANOVA followed by Holm-Sidak test was applied.” (110) “In all statistics, two sided tests were used and $p<0.05$ was considered significant.”(55) “GraphPad Prism software (Version 9, La Jolla, CA, USA) and SPSS (Version 25) were used.” (104)

3.10 Ethical approval

“The studies have been approved by all local institutional review boards…. Patients and parents provided written informed consent, children as appropriate and approved by the local institutional review boards.” (104)

4 Results

4.1 Human peritoneal tight junction, transporter and channel expression in health, kidney failure and associated solute transport

4.1.1 Peritoneal morphology and TJ and transcellular ion transporting proteins and channels in CKD5 and PD

In this dissertation I investigated parietal peritoneal tissues from 70 children with normal kidney function, with end stage kidney disease and on peritoneal dialysis to examine the TJ protein distribution and abundance and their association with peritoneal morphology. For further methodological details please refer to Levai et al. 2023. (104)

4.1.2 Peritoneal morphology of children with normal kidney function, CKD and on PD

Our studies demonstrated inflammatory cell infiltration in the peritoneum and activation of fibroblast and profibrotic activity in children with CKD5, together with vascular lumen narrowing. Reduced mesothelial cell coverage and mesothelial-mesenchymal transitioned cells in the submesothelium were present in patients on neutral pH PD fluids with low glucose degradation product content, while the submesothelial layer being more vascularized and infiltrated by inflammatory cells, e.g. macrophages and leukocytes. [Table 1] We limited our studies to the mesothelial monolayer and the arterioles to exclude any analytic bias by peritoneal inflammatory cell infiltration, which have been described to express junction proteins.

Table 1. Digital histomorphometry of the parietal peritoneum of children with normal kidney function, with CKD5 and on PD for 12.8 (IQR 7.9, 21.9) months. (104)

	Controls (n=23)	**CKD 5 (n=23)**	**PD (n=24)**	**p-value***	**CKD5 vs PD+**
Mesothelial coverage (0-6)	5.0 (3.5, 6.0)	5.0 (5.0, 6.0)	3.0 (1.5, 6.0)	**0.04**	0.06
Submesothelial thickness (µm)	250 (150, 400)	325 (213, 395)	307 (265, 503)	0.07	0.30
Submesothelial microvessel density (/mm^2)	80 (56.5, 185)	126 (80, 150)	161 (111,227)	**0.02**	0.24
Lymphatic vessel density (/mm^2)	37.4 (19.9, 54.3)	26.1 (19, 48.2)	22.5, (8.7, 45.9)	0.26	1.0
Diffuse podoplanin staining (% patients)	0	0	21	0.08	0.97
Blood microvessel density (/mm^2)	61 (38, 160)	98 (64, 117)	153 (64, 219)	**0.01**	0.22
Total endothelial surface area (µm^2/um^3)	3.5 (2.1, 4.7)	5.7 (4.3, 7.4)	9.6 (6.1, 13.7)	**<0.0001**	**0.04**
Lymphatic endothelial surface area (µm^2/um^3)	1.4 (1.1, 3.4)	2.2 (1.5, 2.8)	2.4 (1.4, 4.2)	0.59	1.0
Blood microvessel endothelial surface area (µm^2/ µm^3)	1.6 (1.1, 3.4)	3.4 (2.4, 4.5)	7.2 (5.7, 10.8)	**0.0009**	0.05
L/V ratio	0.61 (0.56, 0.77)	0.53 (0.47, 0.66)	0.46 (0.37, 0.61)	**<0.0001**	0.25
ASMA positive cells (% patients)	0	26.1	45.8	**0.002**	0.28
ASMA score (0-3)	0 (0, 0)	0 (0, 1)	1.0 (0, 2)	**0.0004**	0.08
CD45 positive cells (% patients)	0	13	71	**<0.0001**	**<0.0001**
CD45 score (0-3)	0 (0, 0)	0 (0, 1)	1 (0, 2)	**<0.0001**	**<0.0001**
CD68 positive cells (% patients)	0	8.7	58.3	**<0.0001**	**0.0001**
CD68 score (0-3)	0 (0, 0)	0 (0, 1)	1 (0, 2)	**<0.0001**	**<0.0001**
Fibrin deposits (% patients)	0	4.3	16.7	0.07	0.28
EMT positive (% patients)#	0	0	42	**<0.0001**	**0.0003**
EMT (cells/mm^2)#	n.a.	n.a.	25 (18, 53)	**n.a.**	**n.a.**

*L/V ratio = lumen diameter / vessel ratio, ASMA = alpha smooth muscle actin, EMT = epithelial to mesenchymal transition. # Only EMT positive patients included. n.a. = not applicable. * ANOVA/Kruskal-Wallis test as appropriate. +T-test or Mann-Whitney test as appropriate. Data is expressed as median and interquartile range.*

4.2 Tight junction and transcellular transporter protein abundance in the parietal peritoneum in children with normal kidney function, children with CKD5 and on PD

CLDN1 to -5 and CLDN15 and ZO-1, OCL, TriC [Figure 3.], SGLT1, ENaC and PiT1/SLC20A1 [Figure 4.] were consistently detected in mesothelial and arteriolar endothelial cells in parietal peritoneum of children with normal kidney function, with CKD and on PD.

Age-dependency was only present in mesothelial CLDN4 and arteriolar CLDN1 and CLDN2, other studied proteins had similar abundances across age groups, which suggests that age-dependent differences in the peritoneal solute and water transport may primarily be due to the differences in peritoneal vascularization. (21, 104)

CKD5 patients exhibited a higher abundance of peritoneal mesothelial CLDN2 and arteriolar CLDN3 than in healthy controls. In PD patients mesothelial and arteriolar CLDN1 and mesothelial CLDN2 had the highest abundance, while mesothelial and arteriolar CLDN3 [Figure 3] and arteriolar ENaC were lowest [Figure 4].

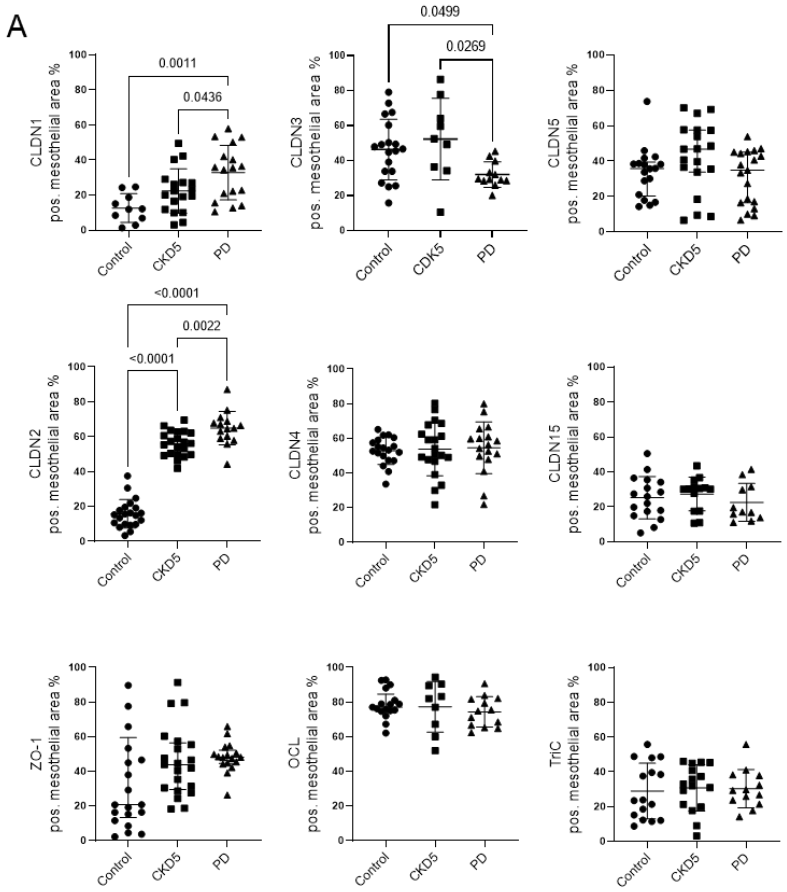

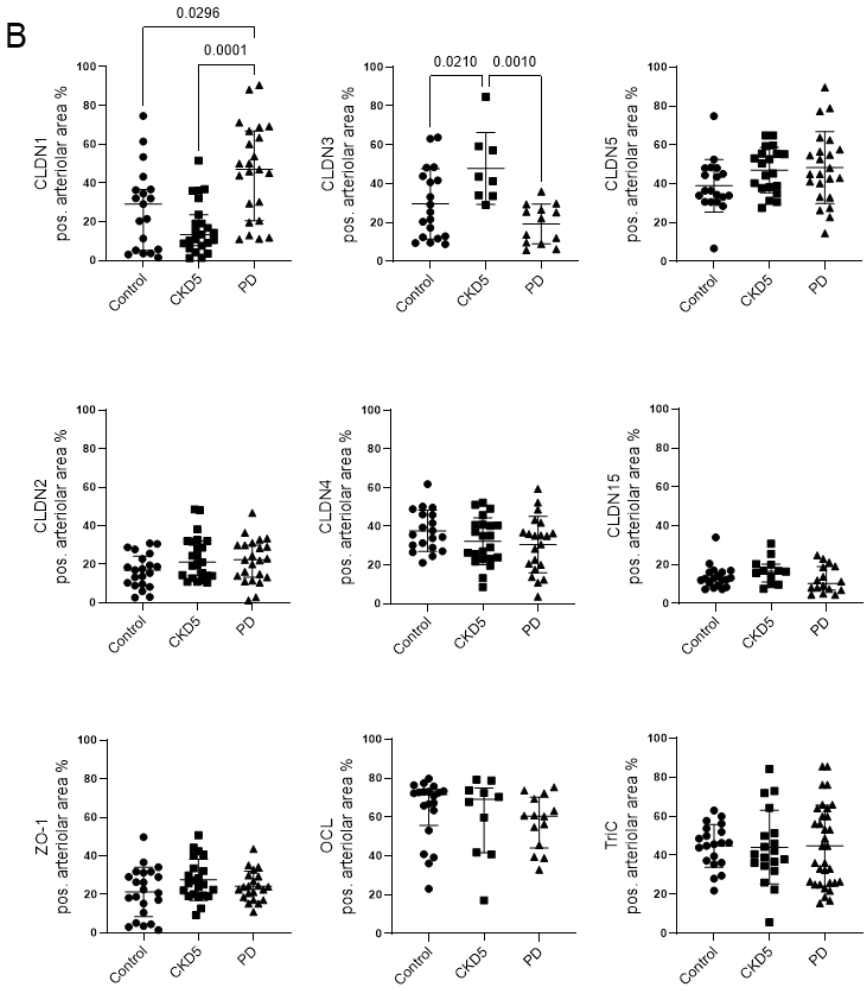

Figure 3. Tight junction protein abundance in children with normal kidney function, children with CKD5 and on PD)

Abundance of sealing claudins (CLDN1, CLDN3, CLND5), pore-forming claudins (CLDN2, CLDN4, CLDN15) and ZO-1, OCL and TriC in the mesothelial (A) and in the arteriolar areas (B). CKD5 patients showed a higher abundance of peritoneal mesothelial CLND1 and arteriolar CLDN2 and -3 than in controls. PD patient samples had the highest mesothelial and arteriolar CLDN1 and mesothelial CLDN2 abundance, while mesothelial and arteriolar CLDN3 were the lowest. Data are presented as median (IQR). One-way ANOVA with Holm-Sidak multiple comparison post-test or Kruskal-Wallis test with Dunn's multiple comparison post-test were used, accordingly. (104)

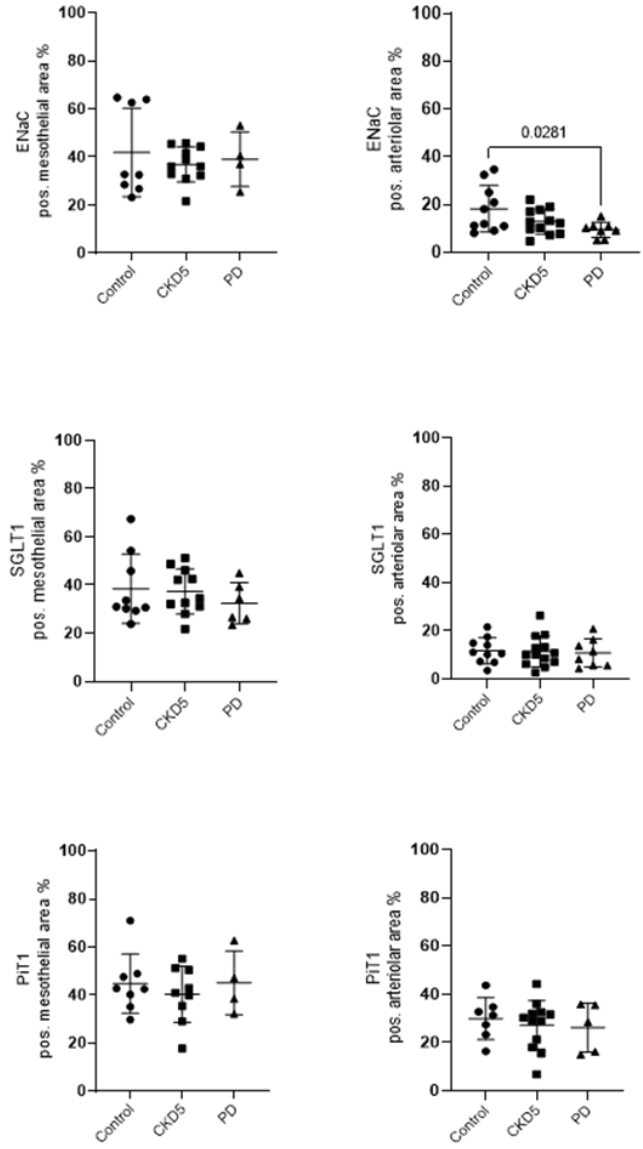

Figure 4. Transcellular sodium channel (ENaC) and sodium and phosphate transporter proteins (SGLT1 and PiT1) in healthy individuals, CKD5 and in PD

Mesothelial ENaC, mesothelial and arteriolar SGLT1 and PiT1 abundance was unchanged over CKD5 and PD treatment. Arteriolar ENaC abundance was lowest in PD, compared to controls. Data are presented median (IQR). Kruskal-Wallis test with Dunn's multiple comparison post-test was used.

In patients with CKD5, peritoneal mesothelial CLDN1 and arteriolar CLDN2 and -3 abundances were higher than in controls. Peritoneum from patients on PD had the highest mesothelial and arteriolar CLDN1 and mesothelial claudin-2 abundance, while mesothelial and arteriolar CLDN3 [Figure 3] and arteriolar ENaC were lowest [Figure 4]. (104)

4.2.1 Peritoneal cellular barrier function in health, CKD and PD

Sealing TJ defines cellular monolayer barrier function, of which endothelial and mesothelial cells are relevant in PD. To study endothelial alterations induced by CKD and PD we analysed parietal arterioles.

Changes in sealing CLDN5/1 ratios have been associated with impaired barrier function in endothelial cells. (68) The peritoneal arteriolar CLDN5/CLDN1 ratio in children with PD was significantly lower (Kruskal-Wallis p=0.002) than in children with normal renal function or CKD. [Figure 5] The findings were not altered by the history of peritonitis.

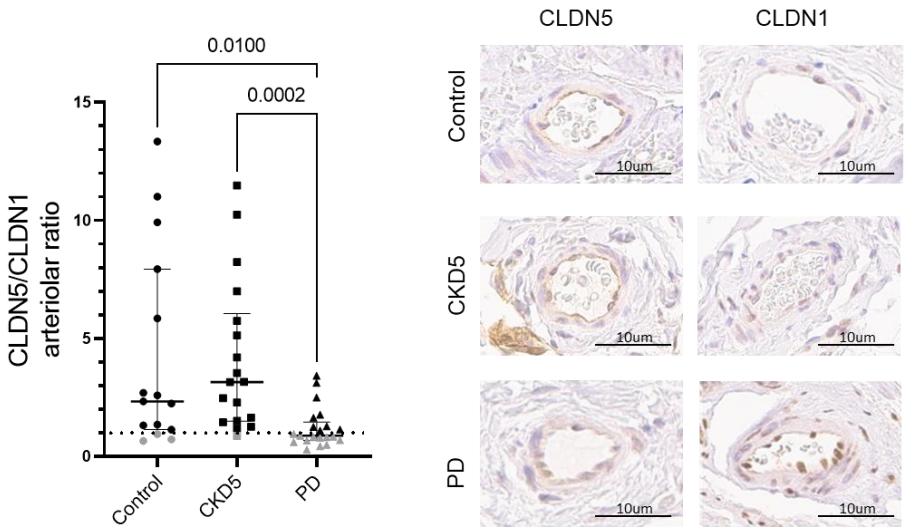

Figure 5. Lower arteriolar CLDN5/CLDN1 abundance ratio in peritoneal dialysis, compared to control and CKD5 indicates an impaired cellular barrier function in PD.

Change of the ratio of arteriolar CLDN5 and CLDN1 sealing proteins due to peritoneal dialysis, indicating an impaired sealing function of the endothelium and sample stainings from all three investigated groups. Data are presented as median (IQR) and Kruskal-Wallis test with Dunn's multiple comparison was used. Representative immunostainings of arterioles are given on the right side. (104) With the permission of Iva Marinovic.

4.2.2 Correlation of tight junction and a transcellular transporter protein with peritoneal membrane solute transport

To understand the putative functional impact of altered transporter protein expression in PD we correlate these with function data obtained in PET tests available in 23 patients. The 2-hour dialysate plasma ratio (D/P_{Crea}= 0.46 ± 0.16) of the creatinine and the 2-hour dialysate glucose/initial dialysate glucose concentration ratios (D/D_0= 0.56 ± 0.21) correlated with arteriolar CLDN2 and mesothelial CLDN15 abundance. In addition, mesothelial CLDN4 correlated with D/D_0 glucose and mesothelial sodium/phosphate cotransporter PiT1 correlated with D/P_{Crea} [Figure 6]. Regarding the arteriolar endothelium, CLDN2 correlations with both $D//D_0$ glucose and D/P_{Crea} has shown a trend, pointing in the same direction ($r = -0.44$, $p = 0.04$; $r = 0.34$, $p = 0.11$), was close near to significance.

öööö9

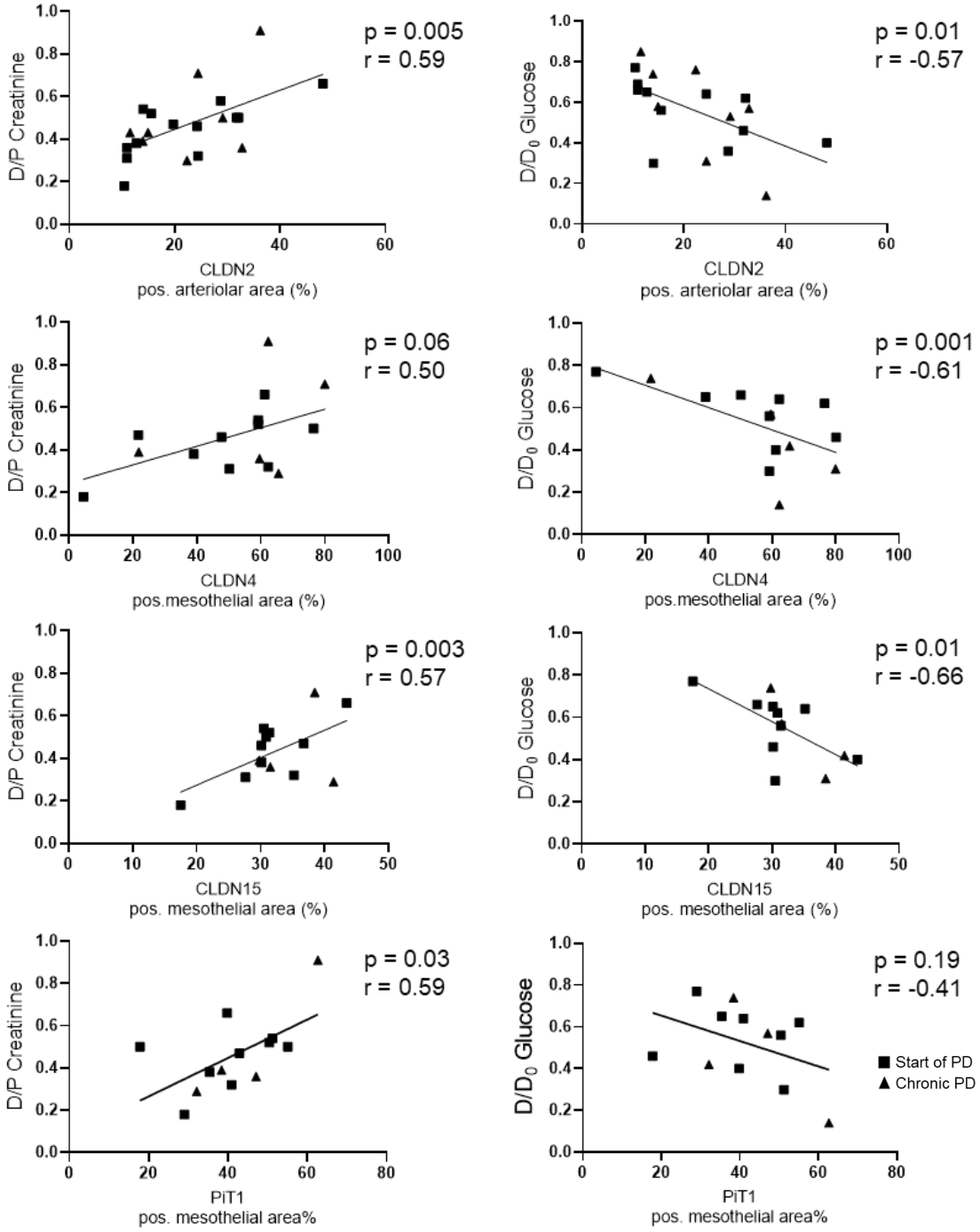

Figure 6. Correlation of arteriolar CLDN2 and mesothelial CLDN4, CLDN15 and PiT1 abundance with D/P_{Crea} and D/D_0 glucose obtained from peritoneal equilibration test data in a subcohort of patients at the start of PD treatment (CKD5) and on chronic PDs. D/P_{Crea} and D/D_0 Glucose significantly correlated with CLDN2 in the arteriolar area, CLDN15 in the mesothelial area and D/D_0 Glucose with CLDN4 (with D/P_{Crea} p=0.06, r=0.50) in mesothelium and D/P_{Crea} with PiT1 (with D/D_0 glucose p=0.19, r=-0.41). (104)

In a multivariable analysis of arteriolar CLDN2 abundance, submesothelial vessel density (quantified by CD31 positivity) and age, solely arteriolar CLDN2 predicted D/P_{Crea} and D/D_0 glucose ratios (p = 0.086/0.036) [Table 2]

Table 2. Multivariable linear regression of D/P_{Crea} (A) and D/D_0 glucose (B) in CKD5 and PD patients with peritoneal equilibration test (PET) data (n=22). (104)

A)

	Multivariable Analysis	
	Coeff. (95% CI)	**p-value**
Microvessel density (/ mm^2)	0.000 (-0.001, 0.001)	0.413
Age (years)	-0.007 (-0.018, 0.004)	0.218
Arteriolar CLDN2 (% pos. area)	0.006 (-0.001, 0.013)	0.086

B)

	Multivariable Analysis	
	Coeff. (95% CI)	**p-value**
Microvessel density (/ mm^2)	0.000 (-0.001, 0.001)	0.664
Age (years)	0.004 (-0.011, 0.018)	0.600
Arteriolar CLDN2 (% pos. area)	-0.010 (-0.018, -0.001)	**0.036**

4.3 Experimental workflow to study protein expression and transport function in a single, polarized cell monolayer

Until now, physiological studies and imaging analyses were performed from different populations of cells, because of different sample preparation techniques required for confocal microscopy, transmission electronmicroscopy or freeze fracture electron microscopy.

We have therefore established an experimental workflow for human umbilical vein endothelial cells (HUVECs), that were cultured on Transwell filters to ensure polarization and performed transendothelial electrical resistance (TER) and FITC dextrane (10 kDa) flux measurements in paralell. In addition to these functional measurements, the same monolayers underwent immunolabeling (ZO-1 and CLDN5), and automated immunofluorescent imaging covering large monolayer areas. Finally, the same monolayers were used for single molecule localization microscopy (SMLM), allowing for ZO-1 and CLDN5 spatial clustering analysis on the nanoscale. [Figure 7.]

Dipeptide Alanyl-Glutamin (AlaGln) was used to modulate the properties of the endothelial monolayers, SMLM showed the non-random, higher degree of clustering of CLDN5 cell-cell junction areas (55, 111).

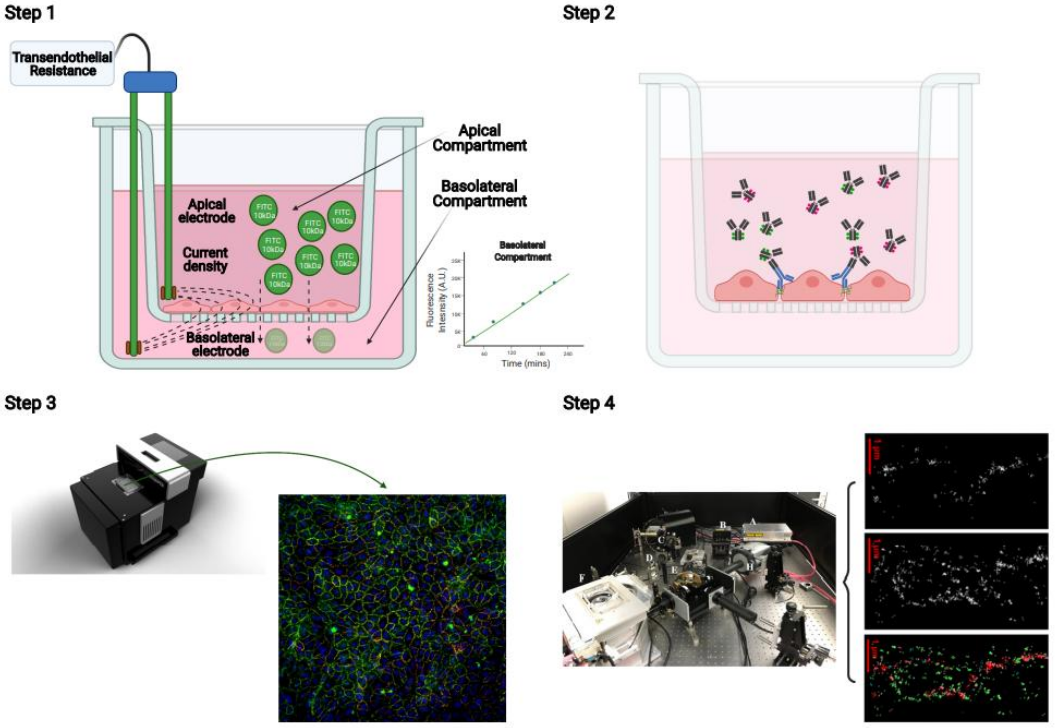

Figure 7. Integration of the stepwise experimental workflow for in-depth TJ study in endothelial cells. HUVECs were grown on PC Transwell filters, and the TER of the monolayer was measured with a volt/ohm meter until confluence. (Step 1): After confluent monolayer formation, experimental solutions were added and TER changes along with 10kDa FITC dextran paracellular transport were monitored for a 4-hour period. (Step 2): Subsequent immunofluorescent staining was performed on the monolayer in the PC Transwell filter with different fluorescently labeled antibodies. (Step 3): Automated immunofluorescence intensity analysis was performed from a z-stacks by the ACQUIFER Imaging Machine comprising 10% of the entire insert. (Step 4): The same filter was subjected to single molecule localization microscopy (SMLM) followed by image processing of the junction area. Image processing algorithms were employed in order to assess the clustering of the TJ proteins of interest. The Figure was constructed with BioRender.com (accessed on 17 March 2021). (111) With the permission of Maria Bartosova.

4.4 Alanyl-Glutamine restores endothelial ZO-1 organization after disruption by a conventional peritoneal dialysis fluid

Next, we analyzed in impact of PD fluid additive AlaGln in stabilizing endothelial integrity and function. AlaGln supplementation to the cell culture medium dose-dependently increased TER in HUVEC. [Figure 8A]

Paracellular barrier's integrity is well reflected by TER in the leaky endothelia. The main tight junction component responsible for this function is ZO-1, a connector of claudins and the actin-cytoskeleton, and in endothelial membranes CLDN5, a key sealing junction protein. (73, 78) The abundance of ZO-1 was reduced with the addition of AlaGln, while CLDN5 abundance increased with 8 mM AlaGln (pharmacological doses used in recent clinical trials) and decreased with administrating higher concentrations of AlaGln [Figure 8BC]. (118)

AlaGln dose-dependently reduced 10 kDa and 70 kDa dextran transport across the HUVEC monolayer. Adding 8 mM AlaGln to the medium, significantly decreased 70 kDa transport across the barrier ($p=0.03$), 10 kDa transport was unchanged ($p=0.15$) (55).

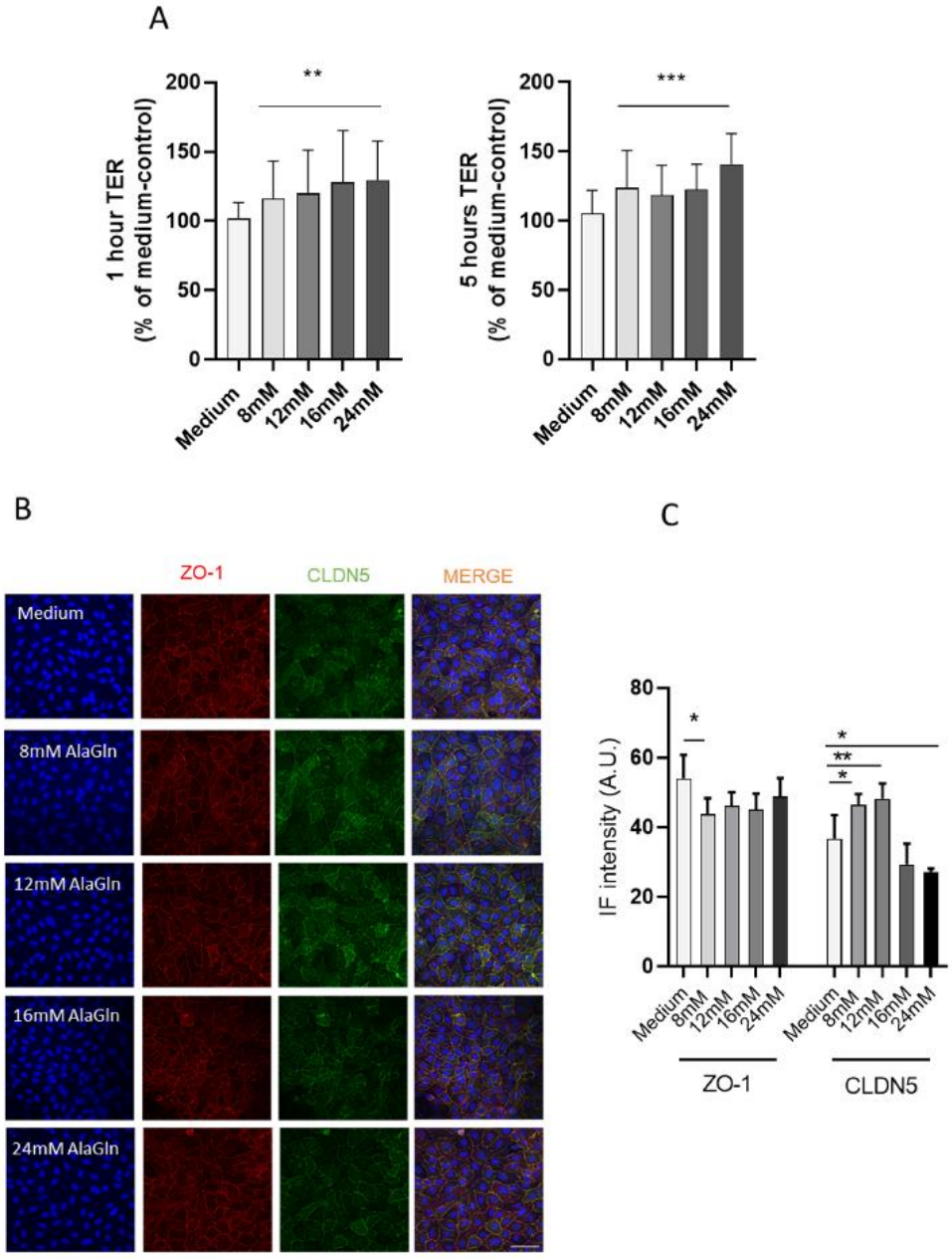

Figure 8. (**A**) Alanyl-glutamine (AlaGln) in cell medium dose-dependently increased TER in human umbilical vein endothelial cells (HUVEC) (ANOVA $p < 0.001$). (**B**) gives representative ZO-1 and CLDN5 stainings of HUVEC treated with increasing doses of AlaGln. Scale bar = 50 µm, (**C**) the mean and SD values of the fluorescence signal quantification of both endothelial junction proteins. Endothelial ZO-1 abundance is decreased and CLDN5 increased with 8 mM AlaGln. A.U.= arbitrary units. * $p < 0.05$, ** $p < 0.01$, *** $p < 0.001$. X axis is signaling doses of AlaGln at both A and C graphs. (55)

Next, endothelial cells were exposed to conventional PD fluids (CPDF) and low GDP PD fluids (LPDF) with or without 8 mM AlaGln. TER increased with AlaGln addition to both CPDF and LPDF, compared to only dialysate fluid treatments. [Figure 9A] Transendothelial transport for 10kDa and 70 kDa molecules was reduced with AlaGln supplemented to CPDF (p = 0.02/0.04), but not in case of LPDF (p = 0.51/0.55) [Figure 9B].

The abundances of ZO-1 and CLDN5 were reduced with incubation of HUVEC with CPDF 9.5 ± 2.2% and 45 ± 12% of medium control, (p = 0.0049/0.02) and addition of 8 mM AlaGln could preserve both ZO-1 and CLDN5 levels 87 ± 23% and 129 ± 69% of medium, (p= 0.54/0.007 vs. medium/CPDF only and p= 0.56/0.05 vs. medium/CPDF only). ZO-1 and CLDN5 abundance was not modified significantly by neither LPDF, nor AlaGln supplemented LPDF incubation (ZO-1: 98 ± 28% and 105 ± 30% of medium control; (p = 0.91/0.78 vs. medium control), CLDN5: 118 ± 47% and 105 ± 25% of medium control, (p = 0.83/0.61 vs. medium control) [Figure 9C].

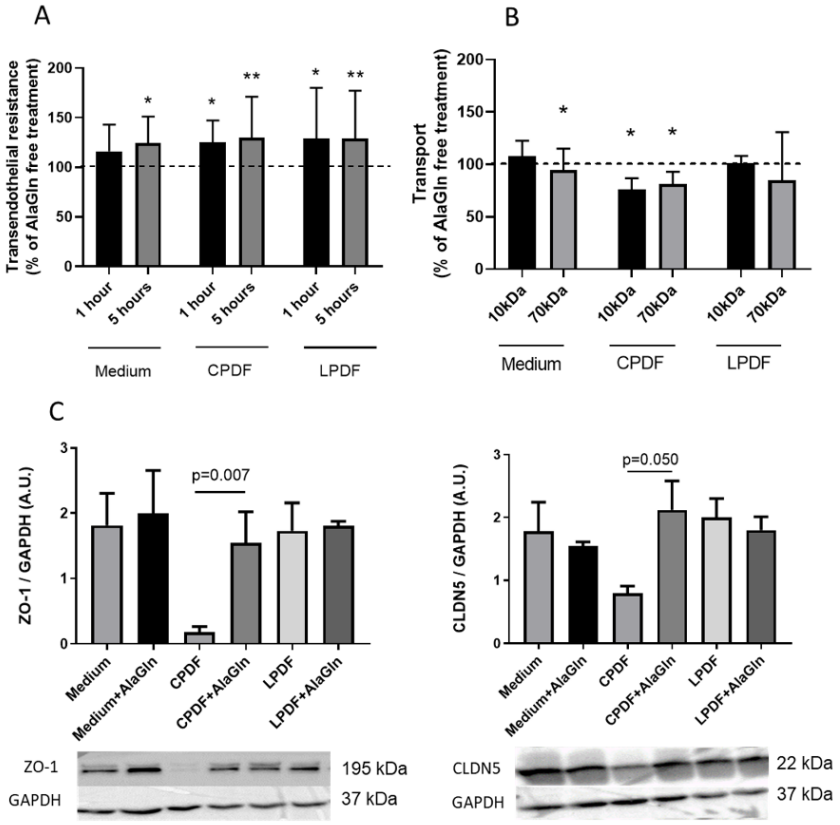

Figure 9. Supplementation of 8 mM alanyl-glutamine (AlaGln) to CPDF and LPDF increased electrical resistance of HUVEC after 1 and 5 h (**A**). 10 kDa and 70 kDa dextran transport was reduced with CPDF only (**B**). Reduction of ZO-1 and CLDN5 protein abundance in CPDF treated HUVEC was restored with AlaGln supplementation (**C**). Data are mean ± SD. A.U. = arbitrary units. * $p < 0.05$, ** $p < 0.01$. (55)

Barrier function, reflected by TER and permeability are defined by the quantity, but also the spatial organization of the intercellular junction proteins. Introduced before, in the experimental workflow to study cell monolayers [Figure 7], we performed SMLM for ZO-1 molecules in cell-cell junction membrane areas. (111)

Consistent to the HUVEC immunofluorescent stainings [Figure 8B], the determined membrane-bound ZO-1 molecule number per nm^2 (determined by the labeling signal density) was reduced with the supplementation of 8 mM AlaGln ((1.39 ± 0.43) × 10−4 counts/nm2 vs. (2.04 ± 0.58) × 10−4 counts/nm2 without AlaGln, (p = 0.01)). There was a significant increase, when AlaGln was supplemented to LPDF ((2.07±0.52)×10−4 counts/nm2 vs. (1.48 ± 0.48) × 10−4 counts/nm^2 without AlaGln, (p = 0.009)). The number of membrane-bound ZO-1 molecules remained unchanged when the same dose of AlaGln was added to CPDF (1.10 ± 0.55) × 10−4 counts/nm2 with AlaGln vs. (1.40 ± 0.71) × 10−4 counts/nm2 without AlaGln, (p= 0.23) [Figure 10A].

Another important aspect of the ZO-1 molecule's relationship to the membrane structure is the spatial, structural organization of it. We examined the membrane regions according to Ripley's distance frequency curve shapes, where occurring peaks indicate the formation of molecular clusters, signaling the functionality of membrane embedded molecules. (119) "The slope of the Ripley curves at higher distances can be used as a measure for the degree of randomness of the surrounding points (120)." (55)

AlaGln supplemented to medium reduced ZO-1 molecule density was accompanied by a slight increase in molecule clustering, reflecting the more homogenous molecule distribution. During incubation with CPDF, AlaGln supplementation strongly increased ZO-1 clustering, but the randomness of the surrounding (i.e. the slope of the Ripley curves at high distances), did not change. Therefore, in case of AlaGln supplementation in medium and CPDF, the increased cluster formation could be related to different density changes. Supplementing AlaGln to LPDF led to an increase of the ZO-1 molecule density and the reduction of its clustering [Figure 10C, D]). (55)

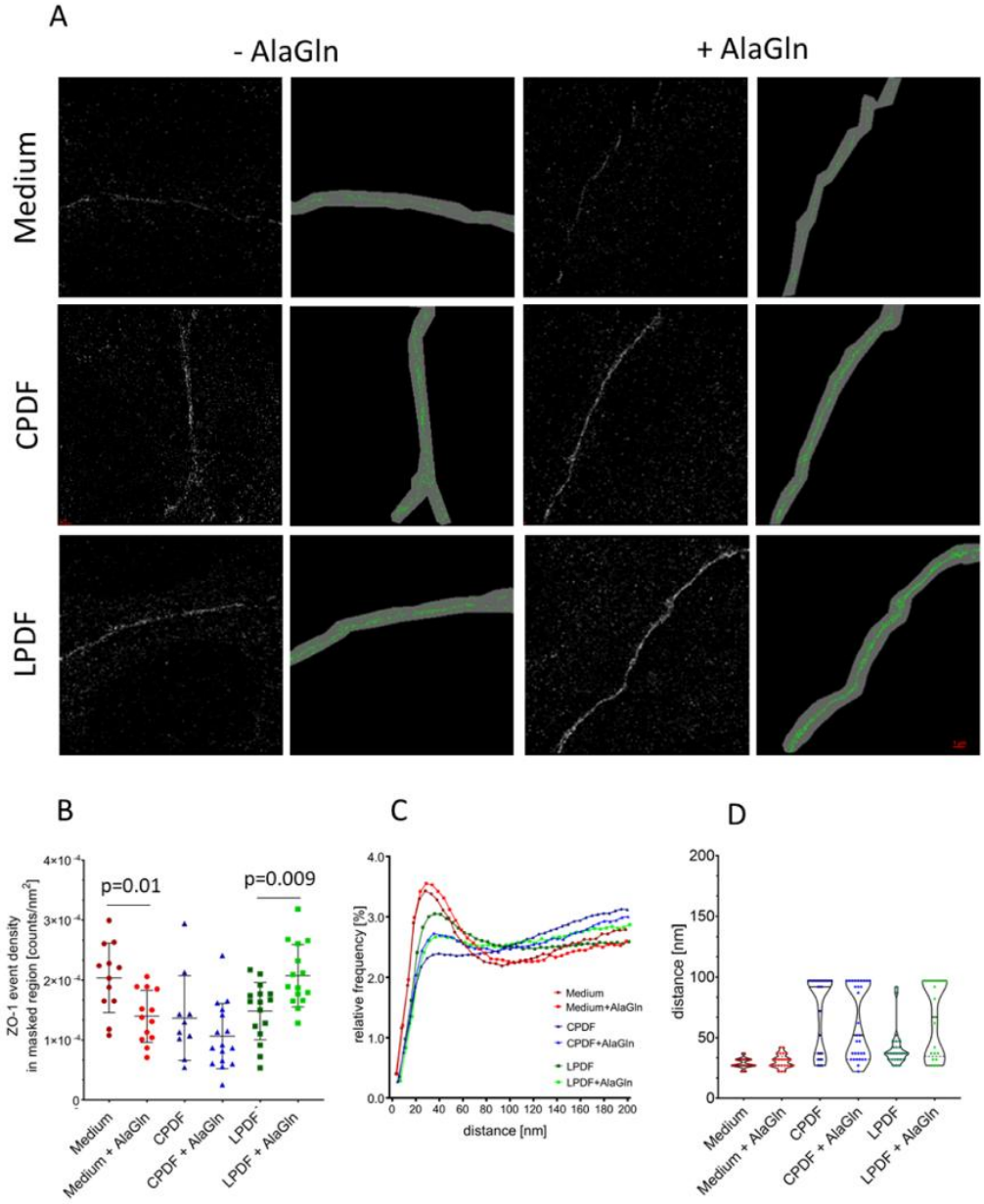

Figure 10. Single molecule localization microscopy was used for quantification and clustering of single ZO-1 molecules at the junction areas in HUVEC, cultured on Transwell filters for proper polarization. Representative localization images reconstructed from the loci data matrix are given in (**A**) with and without masking, mask width is 100 nm (red scale bar = 1 µm). (**B**) ZO-1 molecule density for given treatments, (**C**) Ripley frequency distance curves: relative frequencies of point-to-point distances given on the x-axis (**D**) respective violin plots of the distances at which most molecules were found. Alanyl-glutamine (AlaGln) reduced the number of fluorophore signals in the membrane of endothelial cell incubated with medium and increased it with LPDF incubation (**B**). ZO-1 molecule clustering was changed in a characteristic way when AlaGln was added (**C**,**D**). (55) With the permission of Maria Bartosova.

4.5 GDP induce arteriolar tight junction disintegration

Long-term cardiovascular complications are an important aspect of impaired renal function and renal replacement therapies. Reactive metabolites, i.e. uremic toxins in CKD, and the heavy GDP burden of PD can lead to vasculopathy and worsen the cardiovascular outcomes and long-term mortality of children with renal failure. (110, 121)

Arteriolar omics analysis of microdissected omental arterioles of children with a normal kidney function, with CKD and on PD demonstrated the suppression of canonical actin cytoskeleton and tight junction pathways, related to high-GDP exposure. (110) The abundance of peritoneal ZO-1 was not different between the high- and low-GDP groups (110) but correlated with the L/V ratio ($r=-0.52$, $P=0.021$), Casp3 ($r=0.43$, $P=0.061$), p16 ($r=0.54$, $P=0.016$), and IL-6 ($r=0.50$, $P=0.028$). (110)

As described above, the spatial organization of the intercellular junctions is defining the endothelial integrity, we therefore analyzed ZO-1 organization according to Ripley distance frequency curve shapes. High-GDP PD caused an inferior degree of clustering of ZO-1 in arteriolar endothelial cells, suggesting a less dense organization of ZO-1 molecules in the junctional area (Figure 11A), the degree of randomness of the surrounding points was much higher. Measuring the most frequent distances between single ZO-1 molecules, we have found that most frequent distances between single ZO-1 molecules were higher with high-GDP compared with low-GDP exposure (92 [54.5–97] nm versus 34.5 [28.3–42] nm; $P=6.1\times10-9$, Figure 11B). The number of membrane-bound ZO-1 molecules per nm^2 did not differ ([4.33±3.10] 10-6 and [4.68±3.65] 10-6 counts/nm^2, $P=0.70$; Figure 11C)

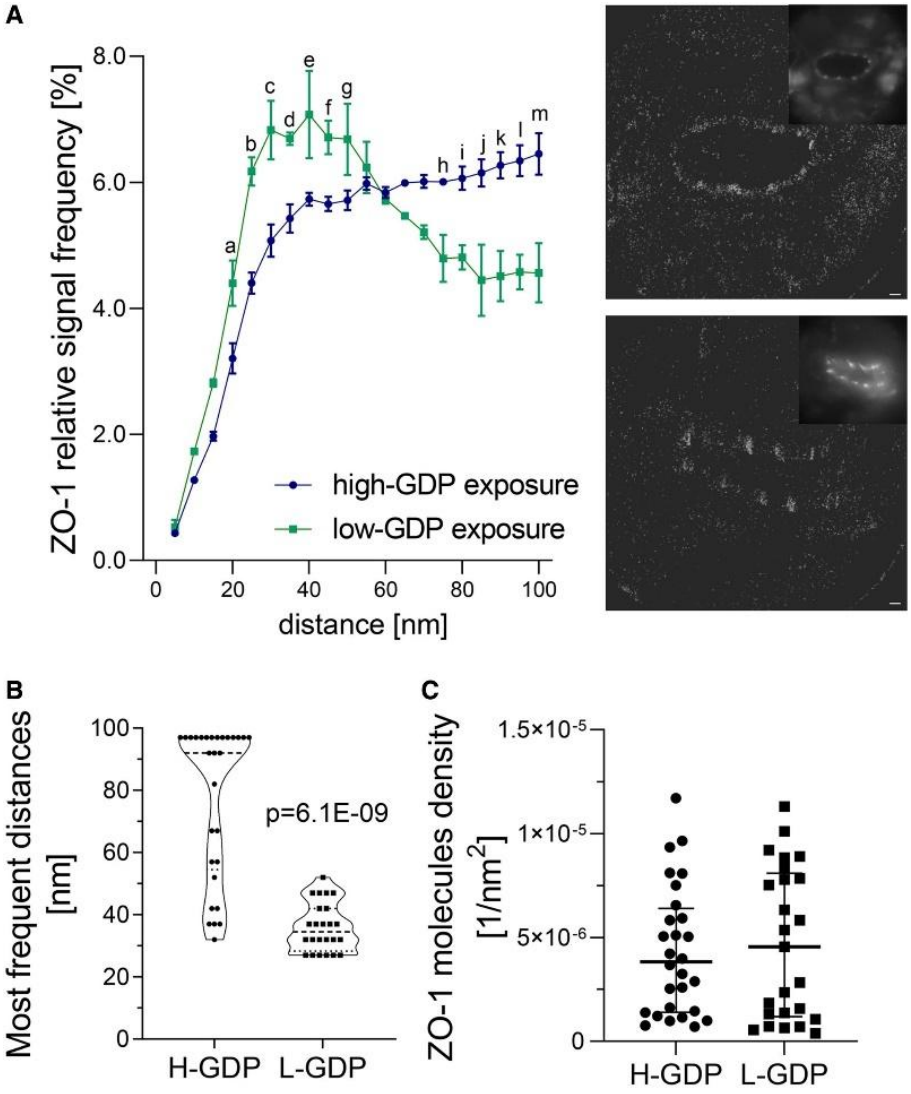

Figure 11. Endothelial ZO-1 (zonula occludens-1) clustering is modified by high–glucose degradation products (H-GDP) PD. A, Single-molecule localization microscopy quantification of ZO-1 clustering within 100 nm distance in parietal peritoneal arteriolar tissue sections of low-GDP (L-GDP)–treated and H-GDP–treated patients (n=3 per group). The representative images on the right give an overview of single arterioles (inset in the upper right corners) and single ZO-1 molecule visualization with H- (upper image) and L-GDP PD (lower image), scale bar=10 µm. Data are presented as median (interquartile range [IQR]), 2-way ANOVA followed by Holm-Sidak test for multiple comparison was applied. Letters indicate significant differences between the groups, individual P values are listed in Table VII in the Data Supplement of Bartosova et al 2021, Circulation Research. **B,** The respective frequencies of the distances between single ZO-1 molecules, (C) the membrane-bound ZO-1 molecules per nm2, n=25. In B and C, data are presented as median (IQR), Mann-Whitney test was applied. (110) With the permission of Maria Bartosova.

Human umbilical arterial endothelial cells (HUAEC) were treated for 24 hours with increasing doses of 3,4-DGE (5, 10, 20 uM content) as present in high-GDP PD fluids. Increasing doses of 3,4-DGE progressively disrupted membrane ZO-1 molecule organization. [Figure12C] Functional studies demonstrated a dose-dependent decline in transendothelial electrical resistance and increased permeability for 4 kDa dextran with 5 to 20 µmol/L 3,4-DGE exposure [Figure 12D].

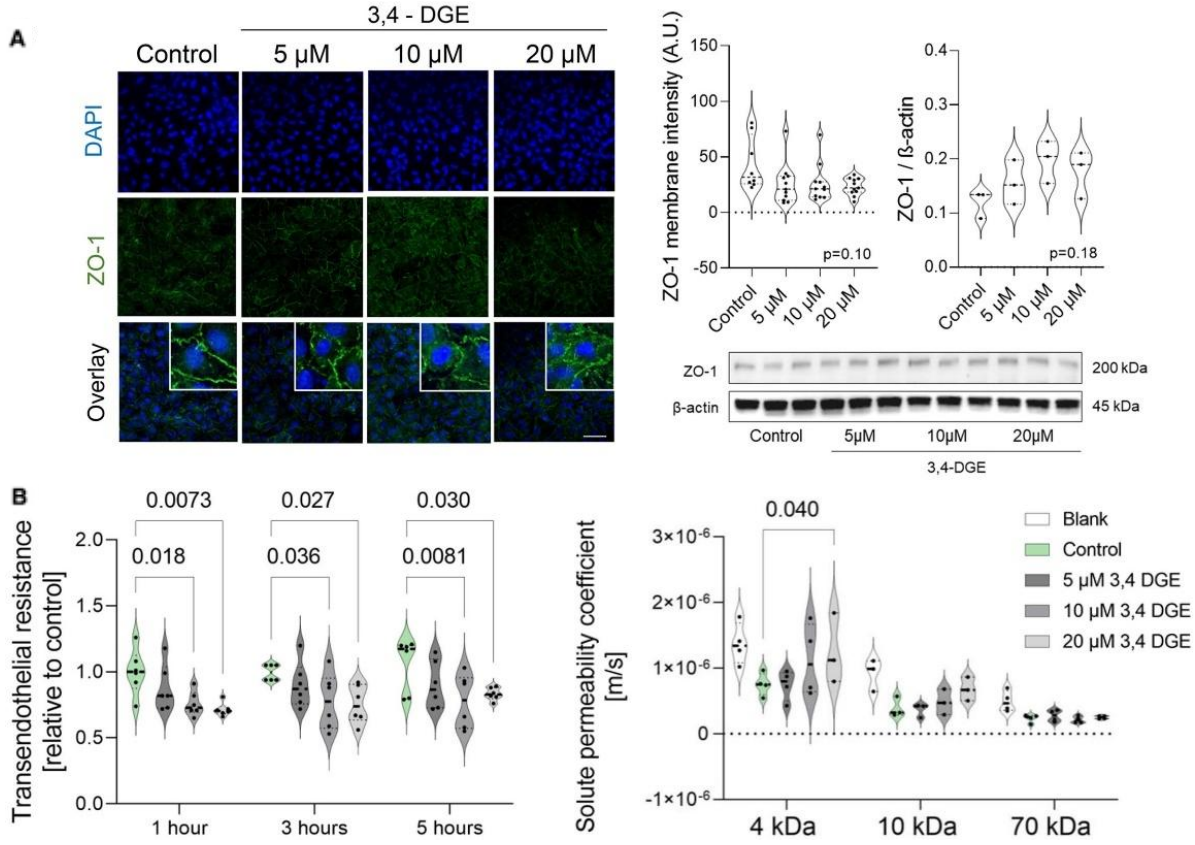

Figure 12. 3,4-dideoxyglucosone-3-ene (3,4-DGE) disrupts membrane ZO-1 (zonula occludens-1) and increases endothelial monolayer permeability. Human umbilical arterial endothelial cells (HUAEC) were incubated with 3,4-DGE at concentrations as present in high–glucose degradation products (GDP) PD fluids for 24 h. A, Total endothelial ZO-1 is unchanged (n=3), cell membrane ZO-1 is disintegrated (n=10). A–B, Analyzed by nonparametric Kruskal-Wallis test). Scale bars=50 µm. B, In Transwells, HUAEC paracellular ionic permeability (transendothelial electric resistance, presented as relative change to medium control, n=6), and 4, 10, and 70 kDa dextran permeabilities in response to increasing concentrations of 3,4-DGE are given (n=6), 2-way ANOVA followed by comparison of treatment vs control group with Holm-Sidak correction was applied. A.U. indicates arbitrary units; DAPI, 4′,6-Diamidin-2-phenylindol; IF, immunofluorescence; and WB, western blot. Adapted from Bartosova et al. Circulation Research 2021. (110) With the permission of Maria Bartosova.

5 Discussion

With the growing prevalence of CKD worldwide together with substantial shortage of kidney donors, the need for improved dialysis care is increasing. This thesis is focused on PD, since it confers several advantages over hemodialysis, especially in the pediatric population, where hemodialysis is hardly feasible in infants and young children. It addresses the thus far largely unresolved question of molecular mechanisms of peritoneal solute transport, the impact of CKD and PD and proofs the concept of future therapeutic modulation to increase PD efficacy and sustainability. (104) The latter are the key shortcomings of current PD therapying children and adults. Another key achievement is the establishment of a standardized in-vitro workflow for a combined in vitro testing of transporter expression and function within one experiment, including SMLM (111) and that PD associated GDP exposure was identified as a key mechanism of endothelial cell junctions and cytoskeleton disruption. (110)

5.1 Human peritoneal tight junction, transporter and channel expression in health, CKD and PD and associated solute transport

The peritoneal membrane is crucial in the abdominal homeostasis and multiple pathological mechanisms (e.g. post-inflammatory and post-interventional adhesions, cancer progression). TJ are fundamentally involved in these processes. (122, 123) The peritoneal membrane goes through progressive alterations through the course of PD due to PD fluid bioincompatibility, limiting its use. (29)

This thesis provides the first comprehensive analysis of barrier forming sealing TJ and pore forming TJ exerting paracellular transport, as well as of the cellular sodium channel ENaC and phosphate and glucose transporters PiT1 and SGLT1 across age groups, and in patients with CKD and on PD. By comparing these findings to the peritoneal solute transport insights functional significance could be obtained, albeit the mechanistic link is not proven.

To underline the importance of not yet described transport proteins, we proved the consistent detectability of CLDN1 to -5 and CLDN15, ZO-1, OCL, TriC, SGLT1 and

PiT1/SLC20A1 in both mesothelial and arteriolar endothelial cells in the parietal peritoneum of children with normal kidney function, with CKD and on PD.

Age-dependency was only present in mesothelial CLDN4 and arteriolar CLDN1 and CLDN2, other findings were consistent among age groups, which suggests that age-dependent differences in the peritoneal solute and water transport may primarily be due to the already known differences in peritoneal vascularization. (21, 104)

Regarding morphological differences among the three groups, CKD increased the peritoneal vessel density, possibly compensating for the arteriolar lumen obliteration also present, just as in previous large-cohort pediatric studies. (21, 104) Even though this effect is already known in peritoneal membrane transformation under uremic conditions, the underlying mechanisms have not yet been studied. In CKD there is a systemic accumulation of uremic toxins, and inflammatory cytokines, oxidative stress is increased, which - according to various in vitro and animal studies – induce the impairment of TJ expression in multiple organs (e.g. intestine, endothelium, liver, kidney, etc.) (122, 124-127) In CKD we observed an increased arteriolar CLDN3 and mesothelial CLDN2 expression. The higher abundance of CLDN2 suggests an impaired barrier function of the mesothelial layer.(28, 61)

In the parietal peritoneum mesothelium and endothelium of PD patients two sealing proteins differed. CLDN1 abundance was increased and CLDN3 was less abundant than in children with CKD. CLDN3 being the only claudin forming complexes with all other proteins of the claudin family. (71, 72) Mesothelial CLDN2 abundance increased further in the PD group of our patients', suggesting a higher deterioration of the barrier function.

ZO-1, OCL and TriC proteins were expressed consistently in the three groups, keeping in mind that the spatial organization of these scaffolding molecules change during CKD and PD (e.g. GDP impact on clustering), influencing the barrier function. (55, 110)

The expressions of ENaC, PiT1 and SGLT1 transcellular transporters and channels, were maintained during CKD5 and PD. [Figure 4]

The overall effect of the TJ regulation on the cellular barrier function is still uncertain, as it is known not to necessarily reflect the function of the TJ complex. The expression, subcellular localization and function of these molecules can differ with cell- and tissue types. (104) (128) The clustering of TJ molecules can reflect paracellular permeability

and is altered e.g. by glucose degradation products present in PD fluids. (55, 104, 110) [Figure 11]

Our findings of an altered arteriolar CLDN5/CLDN1 ratio, due to an altered CLDN1 expression suggests altered vascular sealing in PD. [Figure 5] In CLDN5 deficient mice the blood-brain-barrier (BBB) size-selectively loosens. (129) CLDN5 expressional changes lead to an impaired BBB, and CLDN5 targeted BBB opening is under active investigation for small molecule delivery into the brain. (75, 76) In case of CLDN5 $^{-/-}$ K.O. mice, CLDN12 upregulation can work as a counterbalancing mechanism in the membrane composition. (129) As previously discussed, not only the expression levels, but the spatial organization is important in case of tight junction proteins. (55) In post-ischemic states in mice ischemia/reperfusion models, the inflammatory response inversely correlated with the CLDN5/CLDN1 ratio of the BBB. (67, 68, 130) The role of both claudins and their ratio in peritoneal transport function is yet uncertain. The correlation of CD45 and CD68 cell counts and the CLDN5/CLDN1 ratio was not present in the peritoneum, however the different inflammation patterns induced by PD and in the BBB could be behind this contrast.

Dialytic protein loss is independently predicted by D/P_{Crea} and presence of IL-6 (a marker of local peritoneal inflammation) and may reflect generalized endothelial dysfunction. (131) Addition of AlaGln in a randomized crossover trial reduced peritoneal protein loss. (118) Next to our in vitro results discussed in a later results section, where AlaGln supplementation increased CLDN5 and ZO-1 abundance [Figure 8], clustering and TER in endothelium, our group has also demonstrated that in mice it has upregulated peritoneal CLDN5 expression. (55) All the mentioned findings suggest the significant role of CLDN5 in peritoneal membrane barrier function and thus makes it a good candidate for pharmaceutical targeting.

Despite the chronic disease conditions of CKD and PD, peritoneal membrane transport function should be preserved. PD is a suitable KRT for both children and adults, unless a few contraindications e.g. severe adhesions due to previous surgical interventions. (132) There are certain intraindividual differences in solute transport and transporter status [Figure 2] (45) which are reflected by transport protein differences (133) and peritoneal vascularization as mentioned above and described before in the literature. (21, 29) As a current finding of this dissertation, the transperitoneal transport of creatinine and glucose

correlated with arteriolar CLDN2 and mesothelial CLDN4 and 15, both pore-forming TJ proteins. A correlation between creatinine transport and the mesothelial sodium and phosphate cotransporter, PiT1/SLC20A1 was also detected. [Figure 6] In multivariable analysis, CLDN2 independently predicted peritoneal transport rates. (104) [Table 2]

Based on the latter CLDN2 should be a priority target of therapeutic modulation to enhance peritoneal solute transport.

Correlations between peritoneal membrane transport function and paracellular and transcellular transporters may indicate their role as molecular counterparts in peritoneal transport.

Summarizing these findings, the abundance of paracellular and cellular transporters in healthy controls and changes during CKD and PD in the peritoneum provides a new aspect to find the yet undescribed molecular counterparts of peritoneal membrane function.

Expressional changes in the mesothelial paracellular transport proteins suggest the possible, yet unconsidered role of the mesothelial cell layer in peritoneal transport, thus opening up a wide-range of new possibilities in the preservation of membrane structure and function. (28)

Regarding options of membrane preservation, the effects of acute inflammation on the molecular machinery of peritoneal transport and possible counteractions are central and questions, which we hope to tackle in the future, but is outside the scope of this dissertation.

5.2 Experimental workflow for studying barrier integrity, permeability, and tight junction composition and localization in a single endothelial cell monolayer

In addition to this descriptive work and to be able to model the peritoneal membrane function and study the functional aspects of these membranes, we have established a widely usable workflow, useful for research questions regarding epithelial and endothelial monolayers.

As described previously the “[T]he polarization of endothelial cell monolayers is critical for their absorptive and/or secretory functions as well as the prevention of pathogens entering the systemic circulation. (134, 135) The tight junctions are a dynamic structure

that can be reorganized depending on the external stimuli in a way that the paracellular permeability can adapt to the required characteristics of diffusion restriction. (136) The way claudins interact with other TJ machinery components such as the zonula occludens (ZO) adaptor proteins is an area of great scientific interest and requires methodologies providing functional analyses together with high spatial and temporal resolution. (137) In several pathological conditions, like anaphylaxis or sepsis, the disruption of the endothelial TJ is a hallmark of disease severity and progression since the leakage of proteins to third spaces will follow and induce interstitial and organ oedema that can be fatal for the patient. (138-140) Therefore, a thorough understanding of the mechanisms underlying this disruption and the investigation of potentially therapeutic compounds is of great interest" (111)

The combination of TER, paracellular dextran flux, the estimation of TJ abundance with immunofluorescent labeling and assessing TJ spatial organization with SMLM in endothelial cells make this workflow a uniquely useful approach to obtain coherent data from parallel methods and have an in-depth and comprehensive data from a single endothelial monolayer.

With this workflow it is possible to provide a triad of functional, temporal and spatial description of the paracellular permeability changes that are caused by any stimulus in a single monolayer and affect TJs. (111)

Previously available methodological approaches investigating paracellular permeability in epithelial or endothelial monolayers were limited to assessing only one or two aspects of function. Either TER measurements and paracellular fluxes of fluorescently labelled dextran was available (141-143), without any further highlighting of the underlying molecular mechanisms, or for better visual understanding of TJ localization and abundance changes, immunofluorescence could have been used, or as a further option confocal microscopy performed on a monolayer in a Transwell filter can have an enhanced information content. (143, 144) Using automated imaging techniques enables us to have a high-throughput approach and be able to manage large amount of samples simultaneously in a time-efficient manner. However confocal microscopy, even though it can cover the whole cellular area from apical to basolateral sides with Z-stack imaging, can easily result in fluorophore bleaching, limiting its further use because of higher laser power need for visualization with SMLM microscopy. (145) [Figure 10]

Another classically used method – TEM is not suitable for data collection from multiple perspectives, due to the sample preparation procedure restraints. (80, 146)

Recent progress in SMLM studies opened new opportunities for high spatial resolution experiments in TJ studies, compatible with different techniques used prior to the SMLM method, allowing the usage of a single monolayer grown on a Transwell filter for multidimensional measurements. (55, 147)

"Our experimental workflow provides several advantages. Fewer experiments are needed to collect all the relevant results, and this way the variability among experiments using two or three different monolayers is eliminated, and powerful paired statistical analysis can be performed. (148, 149) The issue of reproducibility in life sciences has long been debated and adopting approaches that yield several experimental results from a single experimental setup leads to more robust results and a reduction in the associated costs. Primary cells are usually preferred, but this imposes a pressing need for performing experiments within the first few passages to prevent bias by cell dedifferentiation. (150, 151) … [o]ur experimental workflow is widely applicable in practically all cell types that form monolayers, and paracellular permeability and TJ study is of value, e.g., in epithelial, mesothelial, and endothelial cells. (152) The fact that PC filters were shown to be suitable for this workflow suggests that, with small modification, this workflow could be used in Ussing chamber experiments where Snapwell PC filters are used." (111)

5.3 Alanyl-Glutamine restores tight junction ZO-1 organization after disruption by a conventional PD fluid

The validity of these findings in the aforementioned methodical work were demonstrated by using AlaGln, a dipeptide that has a sealing effect in endothelial cells. (55)

Recently a clinical trial has demonstrated the improvement of peritoneal membrane semipermeability with the supplementation of AlaGln to peritoneal dialysis fluid, i.e. protein losses were reduced and small solute transport rates increased. (118)

In this work, first we provided experimental evidence that CPDF with AlaGln addition increases the abundance of CLDN5, a sealing junction protein and ZO-1, a scaffolding tight junction protein, regulating barrier function in the endothelial membrane. [Figure 8, Figure 9]

“Tight junctions do not form linear structures along the neighboring endothelial cell membranes as suggested by immunofluorescence microscopy studies but cluster in modifiable functional units. (153) In our experimental setting addition of AlaGln to CPDF increased the clustering of ZO-1, the TER and reduced 10 kDa and 70 kDa dextran transport. [Figure 9B] Thus, AlaGln increases peritoneal endothelial junction expression and spatial organization and functionally reinforces the barrier function. Of note, SMLM were obtained from HUVEC grown on Transwell filters to establish endothelial cell apical and basolateral polarization. In this novel setting, up to now, adequate single molecule distinction could be achieved for ZO-1, but not for CLDN5. [Figure 10]

Supplementation of 8 mM AlaGln to culture medium reduced scaffolding ZO-1 and increased sealing protein CLDN5 abundance, the net effect was an increased TER. In line with this, 70 kDa dextran transport was reduced as compared to control and SMLM demonstrated reduced ZO-1 molecule number in the membrane area, but preserved clustering of ZO-1. [Figure 10] The strong suppression of endothelial cell ZO-1 abundance by CPDF is a novel finding. Reduction of ZO-1 abundance by CPDF has previously been reported in effluent mesothelial cells. (83) In intestinal epithelial cells glutamine regulates ZO-1 abundance and TER (154), and supplementation of AlaGln mitigates toxin induced loss of membrane ZO-1 and of TER. (155) Proteome analysis of mesothelial cells exposed to CPDF suggests actin cytoskeleton disruption (156), but preservation of the cytoskeleton if supplemented with AlaGln. (157) We now provide first evidence that CPDF induced loss of endothelial cell integrity and barrier function can prevented by concomitant AlaGln treatment.”(55)

In the same body of work, not discussed in detail in this dissertation, these findings were also complemented with a murine model. CPDF was administered twice daily in a mouse model, and 10 kDa and 70 kDa dextran transport was reduced. AlaGln addition reduced the collagen deposition induced in the submesothelial space by CPDF (158) and increased peritoneal endothelial CLDN5 abundance. (55)

“Whether peritoneal TJ abundance has an impact on peritoneal membrane transport characteristics is not yet proven. In leaky tissues TER reflects mainly the paracellular barrier, built by TJs and indirect evidence provided by electrophysiology experiments in sheep and human peritoneum suggest that its permeability is reflected by changes in the TER. (51, 52, 159)” (55)

An important “limitation of our study regards the use of human umbilical vein endothelial cells. They are a well-established model in PD research (57), but might not reflect the expression and regulation of junctions in human peritoneal capillary endothelial cells. On the other hand, we were able to reproduce the in vitro findings in parietal peritoneal endothelial cells in mice, and these findings are in line with the functional findings reported in the clinical trial (118) …

Supplementation of AlaGln to the PDF in the phase 2 clinical trial significantly increased circulating AlaGln concentrations and may directly impact on the endothelial barrier. (118) These findings provide a rationale for in vitro and in vivo studies to investigate whether sealing of the endothelial barrier by AlaGln has an impact on the incidence and severity of peritonitis in patients on PD.” (55) By the supplementation of AlaGln to CPDF, the increased barrier function of the endothelium could be reached by the modification of the protein abundance and clustering of the components the TJ complex. “Our studies provide first evidence that targeting of the molecular structures defining peritoneal membrane barrier and transport function may allow to optimize PD efficacy and thus to improve PD sustainability and ultimately patient long-term outcome.” (55)

5.4 GDP load induce systemic PD-associated vasculopathy through endothelial cell junction and cytoskeleton disruption

As the last part of this comprehensive work, addressing membrane function in peritoneal dialysis and in previous disease states, we wanted to focus on systemic effects of GDP burden on vascular endothelial function in high- and low-GDP PD patients and in CKD and to see the consequential effect of the endothelial membrane function changes important in PD complications.

Reactive metabolites, playing a key role in the aging process, aging-related disorders, accumulating in CKD, or reactive glucose metabolites - causal players in the long-term complications of diabetes mellitus still raise uncertainty in the magnitude of their impact on actual patient outcome. (160-164) In peritoneal dialysis high concentrations of reactive metabolites are present in conventional PD fluids (e.g. methylglyoxal, 3,4-DGE – highly reactive dicarbonyl compounds). The debate on whether it is feasible to reach improved outcomes with low-GDP PD fluids is still undecided and high-GDP PD fluids are still

widely used. (165, 166) In this experimental study we provided evidence that GDP plays a fundamental role in arteriolar remodeling.

Systemic effects of PD fluids were studied by choosing the arterioles analyzed in this study to be surrounded by at least 1 mm of fat tissue in the omentum, as it is known that the metabolic tissue stress of PD fluids decline with penetration depth (e.g. 90% of osmotic gradient of PD fluids dissipate in the superficial 400 um of the peritoneal membrane). (167) As in all the former studies we carefully selected our pediatric patients, devoid of confounding lifestyle-related factors, and with an emphasis on no underlying diseases affecting vascular integrity. Only the PD-associated GDP load differed in our groups.

Not discussed in detail in this dissertation, the cross omics approach in omental arterioles revealed "the upregulation of genes and proteins involved in cell death and apoptosis and deactivation of cell viability and survival, cytoskeleton and junction organization, and immune response biofunctions" (110) in omental arterioles exposed to high GDP concentrations, compared to both patients before start of dialysis therapy and patients on low-GDP PD. Differences between pre-PD and low-GDP PD patients in transcriptional patterns were insignificant.

To be able to validate the changes related to GDP-exposure in omental arterioles, it was important to reproduce these findings in parietal peritoneal arterioles, exposed to increased glucose concentrations, as direct effects of PD fluid usage. GDP exposure increased lumen-narrowing and endothelial cell loss. (110)

Addressing the differences between dialytic glucose- and dialytic GDP loads, the glucose load was not significantly different between low- and high-GDP PD patients, however dialytic GDP load was 4- to 12-fold higher in high-GDP PD patients. AGE forming from GDP is through nonenzymatical binding to proteins and lipids, as GDPs are rapidly absorbed and not metabolized to a major extent. (29) As potent glycating agents, GDPs are orders of magnitude more reactive than glucose (e.g. methylglyoxal is 50 000x more reactive). (168) In our arterioles studied AGE abundance was 2- to 3-fold increased, coinciding with 20% higher circulating AGE concentrations associated with high-GDP PD fluid usage. (87, 88)

In vitro GDP load leads to apoptosis of mesothelial cells. (169) In a rat model, administration of methylglyoxal led to vascular AGE deposition, loss of endothelial cells

and narrowing of the lumen. (170) AGE effects through leading to extracellular protein crosslinking, reducing vascular elasticity, RAGE-binding and activation of proinflammatory NF- κB and apoptosis. (171, 172)

We could demonstrate apoptotic activation in omental and parietal arteriolar endothelial cells, for details please refer to our paper Bartosova et al, Circulation Research 2021. (110)

As proven with the invaluable help of our colleagues in the Kirkchoff Institute of Physics "[A]nother mechanism of vasculopathy disclosed by the omics analyses of arterioles relates to the disorganization of the cytoskeleton and cell-cell junctions. ZO-1, an intracellular scaffold protein bridging tight junction claudins to the actin cytoskeleton (77, 173) was not statistically different in abundance in the arterioles with low- and high-GDP exposure. Since junction function depends on spatial molecule distribution, we for the first time applied single-molecule localization microscopy in tissue and demonstrate disruption of the spatial clustering of ZO-1 in the endothelial membrane regions by GDP; the randomness of ZO-1 distribution in the surrounding areas increased. The GDP-related endothelial ZO-1 disruption was reconfirmed in endothelial cells in vitro and resulted in increased paracellular ionic and dextran permeability, that is, disruption of the arterial endothelial cell barrier integrity. The sealing junction CLDN1 was not affected in abundance by GDP but was inversely related with the degree of arteriolar lumen narrowing, again suggesting sealing junction dysfunction as demonstrated for ZO-1." (110) [Figure 11]

In addition to the cytoskeleton disorganization and clustering changes in TJ proteins, in vitro in human umbilical arterial endothelial cells (HUAEC), a proper reference model to human peritoneal capillary endothelial cells we prove a dose-dependent decrease of TER and increase of 4kDa fluorescent dextranes with 3,4-DGE treatment, confirming the loss of endothelial cell integrity and the impaired barrier function of the endothelium. [Figure 12]

With this stepwise approach we have demonstrated the disruptive effect of GDP on multiple levels on the endothelial barrier integrity, as an early step in the multifactorial and gradually progressive development of vasculopathy. (95)

For a detailed discussion of the effects of GDP on the parietal peritoneum, please refer to our article Bartosova et al. Circulation Research, 2021. It has been already reported by

our group that low-GDP fluids positively influence VEGF-A abundance and induce angiogenesis and marked inflammatory cell infiltration. (174) High-GDP fluids mitigate the same processes and peritoneal VEGF-A, IL-6, IL-17 and IL-33 signaling were reduced. (110)

Patients with advanced CKD have exceptionally high risk for cardiovascular complications. (85, 99, 175) Our findings of the GDP-driven induction of multiple vasculopathy-related pathways as demonstrated in omental arterioles, suggest systemic effect,. The advanced lumen narrowing due to high GDP- and glucose exposure in parietal arterioles are of great concern. In this dissertation I performed multiple in vitro TER and fluorescent labeled dextrane flux experiments with Western Blot protein quantifications and immunofluorescent stainings for SMLM microscopy. Based on this data, major GDP induced arteriolas remodelling is demonstrated.

As small arteries and precapillary arterioles regulate peripheral resistance and microcirculation, these findings have a huge clinical relevance and strongly suggest to tailor treatment strategies to reduce systemic GDP load (e.g. low-GDP PD dialysis fluid usage in patients on PD). Further directions of research must address targeting the endothelial dysfunction by either supplementation of dialysis fluids (e.g. AlaGln in Section 4.3 “Finding an additive - Alanyl-Glutamine to restore tight junction organization after disruption by a conventional peritoneal dialysis fluid” section above and in our concerning article (55)) or interventions improving GDP detoxification (55) or by administering scavengers (e.g. histidine-containing peptides resistant to degradation by carnosinase-1. (118)

Therefore, we must redirect attention to GDP overload in CKD and PD influencing long term cardiovascular complications in our patients. Future directions of intervention could be therapeutic options targeting GDP overload in CKD and PD, improving GDP clearence and questioning the use of high-GDP PD fluids to improve vascular endothelial integrity.

6 Conclusions

In this dissertation I have outlined the novel importance of paracellular transport proteins as molecular counterparts of peritoneal membrane function.

By proving consistent detectability and describing the changes of distinct sealing, pore-forming and scaffolding TJ proteins (CLDN1-5, and CLDN15, ZO-1, OCL, TriC) and a few transcellular transporters and channels (PiT1, SGLT1, ENaC), the probable role of these molecules in peritoneal membrane changes during PD was pointed out. Description of mesothelial abundances and changes prepared further functional studies of our group to emphasize the role of the mesothelium as a barrier in peritoneal solute transport. (28)

Finding associations of target TJ molecules and peritoneal membrane transport functional data highlights CLDN2, CLDN4, CLDN15 and PiT1 as possible target molecules for future interventions to enhance PD function.

To standardize and enhance studying barrier integrity, permeability and TJ composition, localization and clustering in a single monolayer, a new experimental workflow was established. Thus, maximizing the retrievable coherent information content from a single monolayer, making it possible for future investigators to provide a triad of functional, temporal and spatial description of paracellular permeability changes, with particular regard to effects on the TJs.

Opening up a window to PD fluid additive research AlaGln was tested and proven to seal the epithelial barrier. Dialysis fluids affect TJ organization by disruption, which can be counteracted by AlaGln through increasing transepithelial resistance and decreasing small and middle molecule transport. Increased CLDN5 and ZO-1 abundance was present with AlaGln supplementation to CPDF and AlaGln also improved the clustering of ZO-1 in the endothelial membrane.

To address further complications of PD treatment and provide a new interface of interventions to molecular counterparts of the endothelial barrier - a link between GDP load and systemic vasculopathy was established. GDP induces endothelial cell junction and cytoskeleton disruption, next to the induction of apoptosis. This finding is crucial for prevention of long-term cardiovascular complications in PD patients, especially children on chronic PD.

7 Summary

Through multiple steps, the potential importance of the investigated para- and transcellular transporters was proven in peritoneal membrane transport. These molecules of interest were consistently detectable in health, and in CKD and PD changes of abundance were described. Peritoneal membrane transport functional data independently correlated with arteriolar CLDN2 abundance, marking it as a potential target molecule for further intervention in PD complications.

For further studies an experimental workflow for studying barrier integrity in monolayers was established. This workflow enables the investigator to uniquely describe the paracellular permeability changes from a functional, temporal and spatial aspect.

By the administration of AlaGln as an additive it was possible to reverse the PD-fluid induced disintegration of the endothelial membrane.

Experiments in the scope of this dissertation pointed out the effect of PD fluid GDP content on endothelial cell junction and cytoskeleton disruption during the process of PD-induced vasculopathy, opening up further opportunities to prevent long-term PD complications.

The investigation of paracellular transport proteins as key players of peritoneal membrane transport function is an important step in understanding peritoneal transport mechanisms and changes during peritoneal dialysis and is pivotal in finding new therapeutical options to improve PD efficacy and to prevent peritoneal membrane changes and systemic PD complications.

8 References

1. Kovesdy CP. Epidemiology of chronic kidney disease: an update 2022. Kidney Int Suppl (2011). 2022;12(1):7-11.
2. Ladanyi E. Krónikus veseelégtelenség
korai diagnosztikájának jelentősége. Hypertonia és Nephrologia. 2023;27(1):23-8.
3. Harambat J, Madden I. What is the true burden of chronic kidney disease in children worldwide? Pediatr Nephrol. 2023;38(5):1389-93.
4. Shi B, Ying T, Chadban SJ. Survival after kidney transplantation compared with ongoing dialysis for people over 70 years of age: A matched-pair analysis. American journal of transplantation : official journal of the American Society of Transplantation and the American Society of Transplant Surgeons. 2023;23(10):1551-60.
5. Zhang Y, Gerdtham UG, Rydell H, Jarl J. Quantifying the Treatment Effect of Kidney Transplantation Relative to Dialysis on Survival Time: New Results Based on Propensity Score Weighting and Longitudinal Observational Data from Sweden. Int J Environ Res Public Health. 2020;17(19).
6. Klomjit N, Kattah AG, Cheungpasitporn W. The Cost-effectiveness of Peritoneal Dialysis Is Superior to Hemodialysis: Updated Evidence From a More Precise Model. Kidney Med. 2021;3(1):15-7.
7. Kidney Disease: Improving Global Outcomes (KDIGO) CKD work group. KDIGO 2012 clinical practice guideline for the evaluation and management of chronic kidney disease. Kidney International Supplements.3:1-150.
8. Harambat J, van Stralen KJ, Kim JJ, Tizard EJ. Epidemiology of chronic kidney disease in children. Pediatr Nephrol. 2012;27(3):363-73.
9. Vivante A, Hildebrandt F. Exploring the genetic basis of early-onset chronic kidney disease. Nature reviews Nephrology. 2016;12(3):133-46.
10. Smith JM, Stablein DM, Munoz R, Hebert D, McDonald RA. Contributions of the Transplant Registry: The 2006 Annual Report of the North American Pediatric Renal Trials and Collaborative Studies (NAPRTCS). Pediatr Transplant. 2007;11(4):366-73.

11. Harada R, Hamasaki Y, Okuda Y, Hamada R, Ishikura K. Epidemiology of pediatric chronic kidney disease/kidney failure: learning from registries and cohort studies. Pediatr Nephrol. 2022;37(6):1215-29.
12. Warady BA, Chadha V. Kidney disease in children: the global perspective. Pediatric Nephrology. 2007;22:1999-2009.
13. Becherucci F, Roperto RM, Materassi M, Romagnani P. Chronic kidney disease in children. Clinical Kidney Journal. 2016;9(4):583-91.
14. KDIGO 2024 Clinical Practice Guideline for the Evaluation and Management of Chronic Kidney Disease. Kidney International. 2024;105(4S):S117-S314.
15. White CT, Gowrishankar M, Feber J, Yiu V. Clinical practice guidelines for pediatric peritoneal dialysis. Pediatr Nephrol. 2006;21(8):1059-66.
16. Reymond MA. Pleura and Peritoneum: the forgotten organs. Pleura Peritoneum. 2016;1(1):1-2.
17. Kunin M, Beckerman P. The Peritoneal Membrane-A Potential Mediator of Fibrosis and Inflammation among Heart Failure Patients on Peritoneal Dialysis. Membranes (Basel). 2022;12(3).
18. Koopmans T, Rinkevich Y. Mesothelial to mesenchyme transition as a major developmental and pathological player in trunk organs and their cavities. Commun Biol. 2018;1:170.
19. Hiriart E, Deepe R, Wessels A. Mesothelium and Malignant Mesothelioma. J Dev Biol. 2019;7(2).
20. Namvar S, Woolf AS, Zeef LA, Wilm T, Wilm B, Herrick SE. Functional molecules in mesothelial-to-mesenchymal transition revealed by transcriptome analyses. J Pathol. 2018;245(4):491-501.
21. Schaefer B, Bartosova M, Macher-Goeppinger S, Ujszaszi A, Wallwiener M, Nyarangi-Dix J, et al. Quantitative Histomorphometry of the Healthy Peritoneum. Sci Rep. 2016;6:21344.
22. Fischer A, Koopmans T, Ramesh P, Christ S, Strunz M, Wannemacher J, et al. Post-surgical adhesions are triggered by calcium-dependent membrane bridges between mesothelial surfaces. Nat Commun. 2020;11(1):3068.

23. Tsai JM, Sinha R, Seita J, Fernhoff N, Christ S, Koopmans T, et al. Surgical adhesions in mice are derived from mesothelial cells and can be targeted by antibodies against mesothelial markers. Sci Transl Med. 2018;10(469).
24. Mutsaers SE, Birnie K, Lansley S, Herrick SE, Lim CB, Prêle CM. Mesothelial cells in tissue repair and fibrosis. Frontiers in pharmacology. 2015;6:113.
25. Jagirdar RM, Papazoglou ED, Pitaraki E, Kouliou OA, Rouka E, Giannakou L, et al. Cell and extracellular matrix interaction models in benign mesothelial and malignant pleural mesothelioma cells in 2D and 3D in-vitro. Clin Exp Pharmacol Physiol. 2021;48(4):543-52.
26. Markov AG, Aschenbach JR, Amasheh S. Claudin clusters as determinants of epithelial barrier function. IUBMB Life. 2015;67(1):29-35.
27. Li J, Chen C, Chen B, Guo T. High FN1 expression correlates with gastric cancer progression. Pathol Res Pract. 2022;239:154179.
28. Iva M, Maria B, Eszter L, Rebecca H, Arslan S, Zhiwei D, et al. Molecular and Functional Characterization of the Peritoneal Mesothelium, a Barrier for Solute Transport. Function. 2024.
29. Schaefer B, Bartosova M, Macher-Goeppinger S, al e. Neutral pH and low–glucose degradation product dialysis fluids induce major early alterations of the peritoneal membrane in children on peritoneal dialysis2018; 94(2):[419-29 pp.].
30. Michels WM, Zweers MM, Smit W, Korevaar J, Struijk DG, van Westrhenen R, et al. Does lymphatic absorption change with the duration of peritoneal dialysis? Perit Dial Int. 2004;24(4):347-52.
31. Tarbell JM. Shear stress and the endothelial transport barrier. Cardiovascular research. 2010;87(2):320-30.
32. Bartosova M, Schaefer B, Vondrak K, Sallay P, Taylan C, Cerkauskiene R, et al. Peritoneal Dialysis Vintage and Glucose Exposure but Not Peritonitis Episodes Drive Peritoneal Membrane Transformation During the First Years of PD. Front Physiol. 2019;10:356.
33. Rippe B. A three pore model of peritoneal transport1993; 13(Supplement 2):[S35-S8 pp.].
34. Zhang W, Freichel M, van der Hoeven F, Nawroth PP, Katus H, Kälble F, et al. Novel Endothelial Cell-Specific AQP1 Knockout Mice Confirm the Crucial Role of

Endothelial AQP1 in Ultrafiltration during Peritoneal Dialysis. PLoS One. 2016;11(1):e0145513.

35. Yang B, Folkesson HG, Yang J, Matthay MA, Ma T, Verkman AS. Reduced osmotic water permeability of the peritoneal barrier in aquaporin-1 knockout mice. The American journal of physiology. 1999;276(1):C76-81.

36. Verkman AS, Yang B, Song Y, Manley GT, Ma T. Role of water channels in fluid transport studied by phenotype analysis of aquaporin knockout mice. Exp Physiol. 2000;85 Spec No:233s-41s.

37. Morelle J, Davies S, Devuyst O. AQP1 Promoter Variant, Water Transport, and Outcome in Peritoneal Dialysis. Reply. The New England journal of medicine. 2022;386(11):1098.

38. Flessner MF. Peritoneal ultrafiltration: physiology and failure. Contributions to nephrology. 2009;163:7-14.

39. Schaefer B, Bartosova M, Macher-Goeppinger S, Sallay P, Voros P, Ranchin B, et al. Neutral pH and low-glucose degradation product dialysis fluids induce major early alterations of the peritoneal membrane in children on peritoneal dialysis. Kidney Int. 2018;94(2):419-29.

40. Ito T, Yorioka N, Yamamoto M, Kataoka K, Yamakido M. Effect of glucose on intercellular junctions of cultured human peritoneal mesothelial cells. J Am Soc Nephrol. 2000;11(11):1969-79.

41. Kaneda K, Miyamoto K, Nomura S, Horiuchi T. Intercellular localization of occludins and ZO-1 as a solute transport barrier of the mesothelial monolayer. J Artif Organs. 2006;9(4):241-50.

42. Gutiérrez-Prieto JA, Soto-Vargas J, Parra-Michel R, Pazarín-Villaseñor HL, García-Sánchez A, Miranda-Díaz AG. The Behavior of the Type of Peritoneal Transport in the Inflammatory and Oxidative Status in Adults Under Peritoneal Dialysis. Front Med (Lausanne). 2019;6:210.

43. Davies SJ, Phillips L, Griffiths AM, Russell LH, Naish PF, Russell GI. What really happens to people on long-term peritoneal dialysis? Kidney Int. 1998;54(6):2207-17.

44. Krediet RT. Acquired Decline in Ultrafiltration in Peritoneal Dialysis: The Role of Glucose. J Am Soc Nephrol. 2021;32(10):2408-15.

45. Warady BA, Alexander SR, Hossli S, Vonesh E, Geary D, Watkins S, et al. Peritoneal membrane transport function in children receiving long-term dialysis. J Am Soc Nephrol. 1996;7(11):2385-91.
46. Chang TI, Kang EW, Lee YK, Shin SK. Higher peritoneal protein clearance as a risk factor for cardiovascular disease in peritoneal dialysis patient. PLoS One. 2013;8(2):e56223.
47. Dong J, Chen Y, Luo S, Xu R, Xu Y. Peritoneal protein leakage, systemic inflammation, and peritonitis risk in patients on peritoneal dialysis. Perit Dial Int. 2013;33(3):273-9.
48. Rajakaruna G, Caplin B, Davenport A. Peritoneal protein clearance rather than faster transport status determines outcomes in peritoneal dialysis patients. Perit Dial Int. 2015;35(2):216-21.
49. Perl J, Huckvale K, Chellar M, John B, Davies SJ. Peritoneal protein clearance and not peritoneal membrane transport status predicts survival in a contemporary cohort of peritoneal dialysis patients. Clin J Am Soc Nephrol. 2009;4(7):1201-6.
50. Balafa O, Halbesma N, Struijk DG, Dekker FW, Krediet RT. Peritoneal albumin and protein losses do not predict outcome in peritoneal dialysis patients. Clin J Am Soc Nephrol. 2011;6(3):561-6.
51. Stefanidis I, Zarogiannis S, Hatzoglou C, Liakopoulos V, Kourti P, Poultsidi A, et al. Enhancement of the transmesothelial resistance of the parietal sheep peritoneum by epinephrine in vitro: ussing-type chamber experiments. Artificial organs. 2005;29(11):919-22.
52. Stefanidis I, Liakopoulos V, Kourti P, Zarogiannis S, Poultsidi A, Mertems PR, et al. Amiloride-sensitive sodium channels on the parietal human peritoneum: evidence by ussing-type chamber experiments. ASAIO journal (American Society for Artificial Internal Organs : 1992). 2007;53(3):335-8.
53. Shen L, Weber CR, Raleigh DR, Yu D, Turner JR. Tight junction pore and leak pathways: a dynamic duo. Annual review of physiology. 2011;73:283-309.
54. Shin K, Fogg VC, Margolis B. Tight junctions and cell polarity. Annual review of cell and developmental biology. 2006;22:207-35.

55. Bartosova M, Herzog R, Ridinger D, Levai E, Jenei H, Zhang C, et al. Alanyl-Glutamine Restores Tight Junction Organization after Disruption by a Conventional Peritoneal Dialysis Fluid. Biomolecules. 2020;10(8).
56. Rippe B, Rosengren BI, Venturoli D. The peritoneal microcirculation in peritoneal dialysis. Microcirculation. 2001;8(5):303-20.
57. Horiuchi T, Matsunaga K, Banno M, Nakano Y, Nishimura K, Hanzawa C, et al. HPMCs induce greater intercellular delocalization of tight junction-associated proteins due to a higher susceptibility to H2O2 compared with HUVECs. Perit Dial Int. 2009;29(2):217-26.
58. Gunzel D, Yu AS. Claudins and the modulation of tight junction permeability. Physiological reviews. 2013;93(2):525-69.
59. Amasheh S, Meiri N, Gitter AH, Schoneberg T, Mankertz J, Schulzke JD, et al. Claudin-2 expression induces cation-selective channels in tight junctions of epithelial cells. Journal of cell science. 2002;115(Pt 24):4969-76.
60. Rosenthal R, Gunzel D, Krug SM, Schulzke JD, Fromm M, Yu AS. Claudin-2-mediated cation and water transport share a common pore. Acta physiologica (Oxford, England). 2017;219(2):521-36.
61. Zeissig S, Bürgel N, Günzel D, Richter J, Mankertz J, Wahnschaffe U, et al. Changes in expression and distribution of claudin 2, 5 and 8 lead to discontinuous tight junctions and barrier dysfunction in active Crohn's disease. Gut. 2007;56(1):61-72.
62. Markov AG, Falchuk EL, Kruglova NM, Rybalchenko OV, Fromm M, Amasheh S. Comparative analysis of theophylline and cholera toxin in rat colon reveals an induction of sealing tight junction proteins. Pflugers Archiv : European journal of physiology. 2014;466(11):2059-65.
63. Paperna T, Peoples R, Wang YK, Kaplan P, Francke U. Genes for the CPE receptor (CPETR1) and the human homolog of RVP1 (CPETR2) are localized within the Williams-Beuren syndrome deletion. Genomics. 1998;54(3):453-9.
64. Kominsky SL, Vali M, Korz D, Gabig TG, Weitzman SA, Argani P, et al. Clostridium perfringens enterotoxin elicits rapid and specific cytolysis of breast carcinoma cells mediated through tight junction proteins claudin 3 and 4. Am J Pathol. 2004;164(5):1627-33.

65. Rosenthal R, Günzel D, Piontek J, Krug SM, Ayala-Torres C, Hempel C, et al. Claudin-15 forms a water channel through the tight junction with distinct function compared to claudin-2. Acta physiologica (Oxford, England). 2020;228(1):e13334.
66. Tebbe B, Mankertz J, Schwarz C, Amasheh S, Fromm M, Assaf C, et al. Tight junction proteins: a novel class of integral membrane proteins. Expression in human epidermis and in HaCaT keratinocytes. Arch Dermatol Res. 2002;294(1-2):14-8.
67. Berndt P, Winkler L, Cording J, Breitkreuz-Korff O, Rex A, Dithmer S, et al. Tight junction proteins at the blood-brain barrier: far more than claudin-5. Cellular and molecular life sciences : CMLS. 2019;76(10):1987-2002.
68. Sladojevic N, Stamatovic SM, Johnson AM, Choi J, Hu A, Dithmer S, et al. Claudin-1-Dependent Destabilization of the Blood-Brain Barrier in Chronic Stroke. J Neurosci. 2019;39(4):743-57.
69. Cherradi S, Ayrolles-Torro A, Vezzo-Vié N, Gueguinou N, Denis V, Combes E, et al. Antibody targeting of claudin-1 as a potential colorectal cancer therapy. J Exp Clin Cancer Res. 2017;36(1):89.
70. Milatz S, Krug SM, Rosenthal R, Günzel D, Müller D, Schulzke JD, et al. Claudin-3 acts as a sealing component of the tight junction for ions of either charge and uncharged solutes. Biochim Biophys Acta. 2010;1798(11):2048-57.
71. Shashikanth N, France MM, Xiao R, Haest X, Rizzo HE, Yeste J, et al. Tight junction channel regulation by interclaudin interference. Nat Commun. 2022;13(1):3780.
72. Schlingmann B, Overgaard CE, Molina SA, Lynn KS, Mitchell LA, Dorsainvil White S, et al. Regulation of claudin/zonula occludens-1 complexes by hetero-claudin interactions. Nat Commun. 2016;7:12276.
73. Amasheh S, Schmidt T, Mahn M, Florian P, Mankertz J, Tavalali S, et al. Contribution of claudin-5 to barrier properties in tight junctions of epithelial cells. Cell Tissue Res. 2005;321(1):89-96.
74. Barmeyer C, Erko I, Awad K, Fromm A, Bojarski C, Meissner S, et al. Epithelial barrier dysfunction in lymphocytic colitis through cytokine-dependent internalization of claudin-5 and -8. J Gastroenterol. 2017;52(10):1090-100.
75. Greene C, Hanley N, Reschke CR, Reddy A, Mäe MA, Connolly R, et al. Microvascular stabilization via blood-brain barrier regulation prevents seizure activity. Nat Commun. 2022;13(1):2003.

76. Vázquez-Liébanas E, Mocci G, Li W, Laviña B, Reddy A, O'Connor C, et al. Mosaic deletion of claudin-5 reveals rapid non-cell-autonomous consequences of blood-brain barrier leakage. Cell Rep. 2024;43(3):113911.
77. Van Itallie CM, Tietgens AJ, Anderson JM. Visualizing the dynamic coupling of claudin strands to the actin cytoskeleton through ZO-1. Mol Biol Cell. 2017;28(4):524-34.
78. Rodgers LS, Beam MT, Anderson JM, Fanning AS. Epithelial barrier assembly requires coordinated activity of multiple domains of the tight junction protein ZO-1. Journal of cell science. 2013;126(Pt 7):1565-75.
79. Günzel D, Fromm M. Claudins and other tight junction proteins. Compr Physiol. 2012;2(3):1819-52.
80. Piontek J, Krug SM, Protze J, Krause G, Fromm M. Molecular architecture and assembly of the tight junction backbone. Biochimica et biophysica acta Biomembranes. 2020;1862(7):183279.
81. Schricker S, Oberacker T, Fritz P, Ketteler M, Alscher MD, Schanz M. Peritoneal Expression of SGLT-2, GLUT1, and GLUT3 in Peritoneal Dialysis Patients. Kidney Blood Press Res. 2022;47(2):125-34.
82. Balzer MS, Rong S, Nordlohne J, Zemtsovski JD, Schmidt S, Stapel B, et al. SGLT2 Inhibition by Intraperitoneal Dapagliflozin Mitigates Peritoneal Fibrosis and Ultrafiltration Failure in a Mouse Model of Chronic Peritoneal Exposure to High-Glucose Dialysate. Biomolecules. 2020;10(11).
83. Retana C, Sanchez E, Perez-Lopez A, Cruz A, Lagunas J, Cruz C, et al. Alterations of intercellular junctions in peritoneal mesothelial cells from patients undergoing dialysis: effect of retinoic Acid. Perit Dial Int. 2015;35(3):275-87.
84. Kim S, Choi EY, Jo CH, Kim GH. Tight junction protein expression from peritoneal dialysis Effluent. Ren Fail. 2019;41(1):1011-5.
85. de Jager DJ, Grootendorst DC, Jager KJ, van Dijk PC, Tomas LM, Ansell D, et al. Cardiovascular and noncardiovascular mortality among patients starting dialysis. Jama. 2009;302(16):1782-9.
86. Schmitt CP, Haraldsson B, Doetschmann R, Zimmering M, Greiner C, Boswald M, et al. Effects of pH-neutral, bicarbonate-buffered dialysis fluid on peritoneal transport kinetics in children. Kidney Int. 2002;61(4):1527-36.

87. Zeier M, Schwenger V, Deppisch R, Haug U, Weigel K, Bahner U, et al. Glucose degradation products in PD fluids: do they disappear from the peritoneal cavity and enter the systemic circulation? Kidney Int. 2003;63(1):298-305.

88. Schmitt CP, von Heyl D, Rieger S, Arbeiter K, Bonzel KE, Fischbach M, et al. Reduced systemic advanced glycation end products in children receiving peritoneal dialysis with low glucose degradation product content. Nephrology Dialysis Transplantation. 2007;22(7):2038-44.

89. Neu AM, Sander A, Borzych-Duzalka D, Watson AR, Vallés PG, Ha IS, et al. Comorbidities in chronic pediatric peritoneal dialysis patients: a report of the International Pediatric Peritoneal Dialysis Network. Peritoneal dialysis international : journal of the International Society for Peritoneal Dialysis. 2012;32(4):410-8.

90. Bartosova M, Schaefer B, Bermejo JL, Tarantino S, Lasitschka F, Macher-Goeppinger S, et al. Complement Activation in Peritoneal Dialysis-Induced Arteriolopathy. J Am Soc Nephrol. 2018;29(1):268-82.

91. Christensen KL, Mulvany MJ. Location of resistance arteries. Journal of vascular research. 2001;38(1):1-12.

92. Utech M, Mennigen R, Bruewer M. Endocytosis and recycling of tight junction proteins in inflammation. J Biomed Biotechnol. 2010;2010:484987.

93. Bojarski C, Weiske J, Schoneberg T, Schroder W, Mankertz J, Schulzke JD, et al. The specific fates of tight junction proteins in apoptotic epithelial cells. Journal of cell science. 2004;117(Pt 10):2097-107.

94. Flavahan NA. In Development-A New Paradigm for Understanding Vascular Disease. Journal of cardiovascular pharmacology. 2017;69(5):248-63.

95. Chistiakov DA, Orekhov AN, Bobryshev YV. Endothelial Barrier and Its Abnormalities in Cardiovascular Disease. Front Physiol. 2015;6:365.

96. Schmitt CP, Aufricht C. Is there such a thing as biocompatible peritoneal dialysis fluid? Pediatr Nephrol. 2016.

97. Schaefer B, Bartosova M, Macher-Goeppinger S, Sallay P, Vörös P, Ranchin B, et al. Neutral pH and low-glucose degradation product dialysis fluids induce major early alterations of the peritoneal membrane in children on peritoneal dialysis. Kidney Int. 2018;94(2):419-29.

98. Srivastava S, Hildebrand S, Fan SL. Long-term follow-up of patients randomized to biocompatible or conventional peritoneal dialysis solutions show no difference in peritonitis or technique survival. Kidney Int. 2011;80(9):986-91.
99. Johnson DW, Brown FG, Clarke M, Boudville N, Elias TJ, Foo MW, et al. The effect of low glucose degradation product, neutral pH versus standard peritoneal dialysis solutions on peritoneal membrane function: the balANZ trial. Nephrol Dial Transplant. 2012;27(12):4445-53.
100. Johnson DW, Brown FG, Clarke M, Boudville N, Elias TJ, Foo MW, et al. Effects of biocompatible versus standard fluid on peritoneal dialysis outcomes. J Am Soc Nephrol. 2012;23(6):1097-107.
101. Nataatmadja MS, Johnson DW, Pascoe EM, Darssan D, Hawley CM, Cho Y. Associations Between Peritoneal Glucose Exposure, Glucose Degradation Product Exposure, and Peritoneal Membrane Transport Characteristics in Peritoneal Dialysis Patients: Secondary Analysis of the balANZ Trial. Perit Dial Int. 2018;38(5):349-55.
102. Mistry CD, Gokal R, Peers E. A randomized multicenter clinical trial comparing isosmolar icodextrin with hyperosmolar glucose solutions in CAPD. MIDAS Study Group. Multicenter Investigation of Icodextrin in Ambulatory Peritoneal Dialysis. Kidney Int. 1994;46(2):496-503.
103. Davies S, Zhao J, McCullough KP, Kim YL, Wang AY, Badve SV, et al. International Icodextrin Use and Association with Peritoneal Membrane Function, Fluid Removal, Patient and Technique Survival. Kidney360. 2022;3(5):872-82.
104. Levai E, Marinovic I, Bartosova M, Zhang C, Schaefer B, Jenei H, et al. Human peritoneal tight junction, transporter and channel expression in health and kidney failure, and associated solute transport. Sci Rep. 2023;13(1):17429.
105. Cano F, Sanchez L, Rebori A, Quiroz L, Delucchi A, Delgado I, et al. The short peritoneal equilibration test in pediatric peritoneal dialysis. Pediatr Nephrol. 2010;25(10):2159-64.
106. Warady BA, Jennings J. The short PET in pediatrics. Perit Dial Int. 2007;27(4):441-5.
107. Twardowski ZJ, Prowant BF, Moore HL, Lou LC, White E, Farris K. Short peritoneal equilibration test: impact of preceding dwell time. Advances in peritoneal dialysis Conference on Peritoneal Dialysis. 2003;19:53-8.

108. Frischmann M, Spitzer J, Funfrocken M, Mittelmaier S, Deckert M, Fichert T, et al. Development and validation of an HPLC method to quantify 3,4-dideoxyglucosone-3-ene in peritoneal dialysis fluids. Biomedical chromatography : BMC. 2009;23(8):843-51.
109. Mittelmaier S, Funfrocken M, Fenn D, Berlich R, Pischetsrieder M. Quantification of the six major alpha-dicarbonyl contaminants in peritoneal dialysis fluids by UHPLC/DAD/MSMS. Analytical and bioanalytical chemistry. 2011;401(4):1183-93.
110. Bartosova M, Zhang C, Schaefer B, Herzog R, Ridinger D, Damgov I, et al. Glucose Derivative Induced Vasculopathy in Children on Chronic Peritoneal Dialysis. Circulation research. 2021.
111. Bartosova M, Ridinger D, Marinovic I, Heigwer J, Zhang C, Levai E, et al. An Experimental Workflow for Studying Barrier Integrity, Permeability, and Tight Junction Composition and Localization in a Single Endothelial Cell Monolayer: Proof of Concept. Int J Mol Sci. 2021;22(15).
112. Kratochwill K, Boehm M, Herzog R, Lichtenauer AM, Salzer E, Lechner M, et al. Alanyl-glutamine dipeptide restores the cytoprotective stress proteome of mesothelial cells exposed to peritoneal dialysis fluids. Nephrol Dial Transplant. 2012;27(3):937-46.
113. Yamamoto N, Yamashita Y, Yoshioka Y, Nishiumi S, Ashida H. Rapid Preparation of a Plasma Membrane Fraction: Western Blot Detection of Translocated Glucose Transporter 4 from Plasma Membrane of Muscle and Adipose Cells and Tissues. Curr Protoc Protein Sci. 2016;85:29.18.1-29.18.2.
114. Hausmann M, Wagner E, Lee JH, Schrock G, Schaufler W, Krufczik M, et al. Super-resolution localization microscopy of radiation-induced histone H2AX-phosphorylation in relation to H3K9-trimethylation in HeLa cells. Nanoscale. 2018;10(9):4320-31.
115. Eryilmaz M, Schmitt E, Krufczik M, Theda F, Lee JH, Cremer C, et al. Localization Microscopy Analyses of MRE11 Clusters in 3D-Conserved Cell Nuclei of Different Cell Lines. Cancers (Basel). 2018;10(1).
116. Lemmer P, Gunkel M, Baddeley D, Kaufmann R, Urich A, Weiland Y, et al. SPDM: light microscopy with single-molecule resolution at the nanoscale. Applied Physics B. 2008;93(1):1.

117. Hausmann M, Ilic N, Pilarczyk G, Lee JH, Logeswaran A, Borroni AP, et al. Challenges for Super-Resolution Localization Microscopy and Biomolecular Fluorescent Nano-Probing in Cancer Research. Int J Mol Sci. 2017;18(10).
118. Vychytil A, Herzog R, Probst P, Ribitsch W, Lhotta K, Machold-Fabrizii V, et al. A randomized controlled trial of alanyl-glutamine supplementation in peritoneal dialysis fluid to assess impact on biomarkers of peritoneal health2018; 94(6):[1227-37 pp.].
119. Boyd PS, Struve N, Bach M, Eberle JP, Gote M, Schock F, et al. Clustered localization of EGFRvIII in glioblastoma cells as detected by high precision localization microscopy. Nanoscale. 2016;8(48):20037-47.
120. Weidner J, Neitzel C, Gote M, Deck J, Küntzelmann K, Pilarczyk G, et al. Advanced image-free analysis of the nano-organization of chromatin and other biomolecules by Single Molecule Localization Microscopy (SMLM). Computational and Structural Biotechnology Journal. 2023;21:2018-34.
121. Hénaut L, Mary A, Chillon J-M, Kamel S, Massy ZA. The Impact of Uremic Toxins on Vascular Smooth Muscle Cell Function. Toxins. 2018;10(6):218.
122. McIntyre CW, Harrison LE, Eldehni MT, Jefferies HJ, Szeto CC, John SG, et al. Circulating endotoxemia: a novel factor in systemic inflammation and cardiovascular disease in chronic kidney disease. Clin J Am Soc Nephrol. 2011;6(1):133-41.
123. Mogi K, Yoshihara M, Iyoshi S, Kitami K, Uno K, Tano S, et al. Ovarian Cancer-Associated Mesothelial Cells: Transdifferentiation to Minions of Cancer and Orchestrate Developing Peritoneal Dissemination. Cancers (Basel). 2021;13(6).
124. Dounousi E, Papavasiliou E, Makedou A, Ioannou K, Katopodis KP, Tselepis A, et al. Oxidative stress is progressively enhanced with advancing stages of CKD. American journal of kidney diseases : the official journal of the National Kidney Foundation. 2006;48(5):752-60.
125. Vaziri ND, Goshtasbi N, Yuan J, Jellbauer S, Moradi H, Raffatellu M, et al. Uremic plasma impairs barrier function and depletes the tight junction protein constituents of intestinal epithelium. Am J Nephrol. 2012;36(5):438-43.
126. Vaziri ND, Zhao YY, Pahl MV. Altered intestinal microbial flora and impaired epithelial barrier structure and function in CKD: the nature, mechanisms, consequences and potential treatment. Nephrol Dial Transplant. 2016;31(5):737-46.

127. Rao R. Oxidative stress-induced disruption of epithelial and endothelial tight junctions. Front Biosci. 2008;13:7210-26.
128. Rahner C, Mitic LL, Anderson JM. Heterogeneity in expression and subcellular localization of claudins 2, 3, 4, and 5 in the rat liver, pancreas, and gut. Gastroenterology. 2001;120(2):411-22.
129. Nitta T, Hata M, Gotoh S, Seo Y, Sasaki H, Hashimoto N, et al. Size-selective loosening of the blood-brain barrier in claudin-5-deficient mice. The Journal of cell biology. 2003;161(3):653-60.
130. Aslam M, Ahmad N, Srivastava R, Hemmer B. TNF-alpha induced NFκB signaling and p65 (RelA) overexpression repress Cldn5 promoter in mouse brain endothelial cells. Cytokine. 2012;57(2):269-75.
131. Yu Z, Lambie M, Chess J, Williams A, Do JY, Topley N, et al. Peritoneal Protein Clearance Is a Function of Local Inflammation and Membrane Area Whereas Systemic Inflammation and Comorbidity Predict Survival of Incident Peritoneal Dialysis Patients. Front Physiol. 2019;10:105.
132. Qureshi MA, Maierean S, Crabtree JH, Clarke A, Armstrong S, Fissell R, et al. The Association of Intra-Abdominal Adhesions with Peritoneal Dialysis Catheter-Related Complications. Clin J Am Soc Nephrol. 2024;19(4):472-82.
133. Morelle J, Marechal C, Yu Z, Debaix H, Corre T, Lambie M, et al. AQP1 Promoter Variant, Water Transport, and Outcomes in Peritoneal Dialysis. The New England journal of medicine. 2021;385(17):1570-80.
134. Sigurbjörnsdóttir S, Mathew R, Leptin M. Molecular mechanisms of de novo lumen formation. Nature Reviews Molecular Cell Biology. 2014;15(10):665-76.
135. Lizama CO, Zovein AC. Polarizing pathways: balancing endothelial polarity, permeability, and lumen formation. Exp Cell Res. 2013;319(9):1247-54.
136. Tsukita S, Tanaka H, Tamura A. The Claudins: From Tight Junctions to Biological Systems. Trends in Biochemical Sciences. 2019;44(2):141-52.
137. Zihni C, Mills C, Matter K, Balda MS. Tight junctions: from simple barriers to multifunctional molecular gates. Nature reviews Molecular cell biology. 2016;17(9):564-80.

138. Looney MR, Matthay MA. Bench-to-bedside review: the role of activated protein C in maintaining endothelial tight junction function and its relationship to organ injury. Crit Care. 2006;10(6):239.
139. Liu Y, Mu S, Li X, Liang Y, Wang L, Ma X. Unfractionated Heparin Alleviates Sepsis-Induced Acute Lung Injury by Protecting Tight Junctions. The Journal of surgical research. 2019;238:175-85.
140. Radeva MY, Waschke J. Mind the gap: mechanisms regulating the endothelial barrier. Acta physiologica (Oxford, England). 2017.
141. Arsenopoulou ZV, Taitzoglou IA, Molyvdas P-A, Gourgoulianis KI, Hatzoglou C, Zarogiannis SG. Silver nanoparticles alter the permeability of sheep pleura and of sheep and human pleural mesothelial cell monolayers. Environmental Toxicology and Pharmacology. 2017;50:212-5.
142. Srinivasan B, Kolli AR, Esch MB, Abaci HE, Shuler ML, Hickman JJ. TEER measurement techniques for in vitro barrier model systems. Journal of laboratory automation. 2015;20(2):107-26.
143. Miyazaki K, Hashimoto K, Sato M, Watanabe M, Tomikawa N, Kanno S, et al. Establishment of a method for evaluating endothelial cell injury by TNF-α in vitro for clarifying the pathophysiology of virus-associated acute encephalopathy. Pediatric Research. 2017;81(6):942-7.
144. Gillespie JL, Anyah A, Taylor JM, Marlin JW, Taylor TA. A Versatile Method for Immunofluorescent Staining of Cells Cultured on Permeable Membrane Inserts. Med Sci Monit Basic Res. 2016;22:91-4.
145. Jonkman J. Rigor and Reproducibility in Confocal Fluorescence Microscopy. Cytometry Part A. 2020;97(2):113-5.
146. Tsukita S, Furuse M, Itoh M. Multifunctional strands in tight junctions. Nature reviews Molecular cell biology. 2001;2(4):285-93.
147. Gonschior H, Haucke V, Lehmann M. Super-Resolution Imaging of Tight and Adherens Junctions: Challenges and Open Questions. Int J Mol Sci. 2020;21(3).
148. Stevens JR, Herrick JS, Wolff RK, Slattery ML. Power in pairs: assessing the statistical value of paired samples in tests for differential expression. BMC Genomics. 2018;19(1):953.

149. Ledolter J, Kardon RH. Focus on Data: Statistical Design of Experiments and Sample Size Selection Using Power Analysis. Investigative Ophthalmology & Visual Science. 2020;61(8):11-.
150. Elaut G, Henkens T, Papeleu P, Snykers S, Vinken M, Vanhaecke T, et al. Molecular mechanisms underlying the dedifferentiation process of isolated hepatocytes and their cultures. Curr Drug Metab. 2006;7(6):629-60.
151. Uhal BD, Flowers KM, Rannels DE. Type II pneumocyte proliferation in vitro: problems and future directions. American Journal of Physiology-Lung Cellular and Molecular Physiology. 1991;261(4):L110-L7.
152. Pongkorpsakol P, Turner JR, Zuo L. Culture of Intestinal Epithelial Cell Monolayers and Their Use in Multiplex Macromolecular Permeability Assays for In Vitro Analysis of Tight Junction Size Selectivity. Current Protocols in Immunology. 2020;131(1):e112.
153. Lynn KS, Peterson RJ, Koval M. Ruffles and spikes: Control of tight junction morphology and permeability by claudins. Biochimica et biophysica acta Biomembranes. 2020;1862(9):183339.
154. Li N, Lewis P, Samuelson D, Liboni K, Neu J. Glutamine regulates Caco-2 cell tight junction proteins. American journal of physiology Gastrointestinal and liver physiology. 2004;287(3):G726-33.
155. Seth A, Basuroy S, Sheth P, Rao RK. L-Glutamine ameliorates acetaldehyde-induced increase in paracellular permeability in Caco-2 cell monolayer. American journal of physiology Gastrointestinal and liver physiology. 2004;287(3):G510-7.
156. Kratochwill K, Lechner M, Siehs C, Lederhuber HC, Rehulka P, Endemann M, et al. Stress responses and conditioning effects in mesothelial cells exposed to peritoneal dialysis fluid. J Proteome Res. 2009;8(4):1731-47.
157. Boehm M, Herzog R, Klinglmüller F, Lichtenauer AM, Wagner A, Unterwurzacher M, et al. The Peritoneal Surface Proteome in a Model of Chronic Peritoneal Dialysis Reveals Mechanisms of Membrane Damage and Preservation. Front Physiol. 2019;10:472.
158. Ferrantelli E, Liappas G, Vila Cuenca M, Keuning ED, Foster TL, Vervloet MG, et al. The dipeptide alanyl-glutamine ameliorates peritoneal fibrosis and attenuates IL-17 dependent pathways during peritoneal dialysis. Kidney Int. 2016;89(3):625-35.

159. Kourti P, Zarogiannis SG, Liakopoulos V, Karioti A, Eleftheriadis T, Hatzoglou C, et al. Endothelin-1 acutely reduces the permeability of visceral sheep peritoneum in vitro through both endothelin-A and endothelin-B receptors. Artificial organs. 2013;37(3):308-12.

160. Nigro C, Leone A, Fiory F, Prevenzano I, Nicolò A, Mirra P, et al. Dicarbonyl Stress at the Crossroads of Healthy and Unhealthy Aging. Cells. 2019;8(7).

161. Nandi A, Yan LJ, Jana CK, Das N. Role of Catalase in Oxidative Stress- and Age-Associated Degenerative Diseases. Oxidative medicine and cellular longevity. 2019;2019:9613090.

162. Schalkwijk CG, Stehouwer CDA. Methylglyoxal, a Highly Reactive Dicarbonyl Compound, in Diabetes, Its Vascular Complications, and Other Age-Related Diseases. Physiological reviews. 2020;100(1):407-61.

163. Koutroumpakis E, Jozwik B, Aguilar D, Taegtmeyer H. Strategies of Unloading the Failing Heart from Metabolic Stress. The American journal of medicine. 2020;133(3):290-6.

164. Busch M, Franke S, Müller A, Wolf M, Gerth J, Ott U, et al. Potential cardiovascular risk factors in chronic kidney disease: AGEs, total homocysteine and metabolites, and the C-reactive protein. Kidney Int. 2004;66(1):338-47.

165. Htay H, Johnson DW, Wiggins KJ, Badve SV, Craig JC, Strippoli GF, et al. Biocompatible dialysis fluids for peritoneal dialysis. The Cochrane database of systematic reviews. 2018;10:Cd007554.

166. Blake PG. Is the peritoneal dialysis biocompatibility hypothesis dead? Kidney Int. 2018;94(2):246-8.

167. Flessner MF, Fenstermacher JD, Dedrick RL, Blasberg RG. A distributed model of peritoneal-plasma transport: tissue concentration gradients. The American journal of physiology. 1985;248(3 Pt 2):F425-35.

168. Tauer A, Bender TO, Fleischmann EH, Niwa T, Jörres A, Pischetsrieder M. Fate of the glucose degradation products 3-deoxyglucosone and glyoxal during peritoneal dialysis. Molecular nutrition & food research. 2005;49(7):710-5.

169. Thornalley PJ. Dicarbonyl intermediates in the maillard reaction. Ann N Y Acad Sci. 2005;1043:111-7.

170. Santamaría B, Ucero AC, Benito-Martin A, Vicent MJ, Orzáez M, Celdrán A, et al. Biocompatibility reduces inflammation-induced apoptosis in mesothelial cells exposed to peritoneal dialysis fluid. Blood purification. 2015;39(1-3):200-9.
171. Berlanga J, Cibrian D, Guillén I, Freyre F, Alba JS, Lopez-Saura P, et al. Methylglyoxal administration induces diabetes-like microvascular changes and perturbs the healing process of cutaneous wounds. Clinical science (London, England : 1979). 2005;109(1):83-95.
172. Fishman SL, Sonmez H, Basman C, Singh V, Poretsky L. The role of advanced glycation end-products in the development of coronary artery disease in patients with and without diabetes mellitus: a review. Molecular medicine (Cambridge, Mass). 2018;24(1):59.
173. Martins F, Sousa J, Pereira CD, da Cruz ESOAB, Rebelo S. Nuclear envelope dysfunction and its contribution to the aging process. Aging cell. 2020;19(5):e13143.
174. Freeman SA, Jaumouillé V, Choi K, Hsu BE, Wong HS, Abraham L, et al. Toll-like receptor ligands sensitize B-cell receptor signalling by reducing actin-dependent spatial confinement of the receptor. Nat Commun. 2015;6:6168.
175. Ribatti D, Ranieri G. Tryptase, a novel angiogenic factor stored in mast cell granules. Exp Cell Res. 2015;332(2):157-62.

9 Bibliography of the candidate's publications

Research articles related to the topic of the PhD-thesis:

1) **Levai E,** Marinovic I, Bartosova M, Zhang C, Schaefer B, Jenei H, Du Z, Drozdz D, Klaus G, Arbeiter K, Romero P, Schwenger V, Schwab C, Szabo AJ, Zarogiannis SG, Schmitt CP. **Human peritoneal tight junction, transporter and channel expression in health and kidney failure, and associated solute transport. Sci Rep. 2023** Oct 13;13(1):17429. doi: 10.1038/s41598-023-44466-z. PMID: 37833387; PMCID: PMC10575882.
2) Bartosova M, Ridinger D, Marinovic I, Heigwer J, Zhang C, **Levai E**, Westhoff JH, Schaefer F, Terjung S, Hildenbrand G, Krunic D, Bestvater F, Hausmann M, Schmitt CP, Zarogiannis SG. **An Experimental Workflow for Studying Barrier Integrity, Permeability, and Tight Junction Composition and Localization in a Single Endothelial Cell Monolayer: Proof of Concept. Int J Mol Sci. 2021** Jul 30;22(15):8178. doi: 10.3390/ijms22158178. PMID: 34360944; PMCID: PMC8347178.
3) Bartosova M, Zhang C, Schaefer B, Herzog R, Ridinger D, Damgov I, **Levai E**, Marinovic I, Eckert C, Romero P, Sallay P, Ujszaszi A, Unterwurzacher M, Wagner A, Hildenbrand G, Warady BA, Schaefer F, Zarogiannis SG, Kratochwill K, Schmitt CP. **Glucose Derivative Induced Vasculopathy in Children on Chronic Peritoneal Dialysis. Circ Res. 2021** Aug 20;129(5):e102-e118. doi: 10.1161/CIRCRESAHA.121.319310. Epub 2021 Jul 8. PMID: 34233458.
4) Bartosova M, Herzog R, Ridinger D, **Levai E**, Jenei H, Zhang C, González Mateo GT, Marinovic I, Hackert T, Bestvater F, Hausmann M, López Cabrera M, Kratochwill K, Zarogiannis SG, Schmitt CP. **Alanyl-Glutamine Restores Tight Junction Organization after Disruption by a Conventional Peritoneal Dialysis Fluid. Biomolecules. 2020** Aug 13;10(8):1178. doi: 10.3390/biom10081178. PMID: 32823646; PMCID: PMC7464725.

Research articles not included in the PhD-thesis:

5) Marinovic I, Bartosova M, **Levai E**, Herzog R, Saleem A, Du Z, Zhang C, Sacnun JM, Pitaraki E, Sinis S, Damgov I, Krunic D, Lajqi T, Al-Saeedi M, Szabo JA, Hausmann M, Pap D, Kratochwill K, Krug SM, Zarogiannis SG, Schmitt CP. **Molecular and Functional Characterization of the Peritoneal Mesothelium, a Barrier for Solute Transport. Function** (Oxf). 2025 Feb 12;6(1):zqae051. doi: 10.1093/function/zqae051. PMID: 39658363; PMCID: PMC11815573.
6) Atikel YÖ, Schmitt CP, **Levai E**, Adalat S, Shroff R, Goodman N, Dursun İ, Pınarbaşı AS, Yazıcıoğlu B, Paglialonga F, Vondrak K, Guzzo I, Printza N, Zurowska A, Zagożdżon I, Bayazıt AK, Atmış B, Tkaczyk M, do Sameiro Faria M, Zaloszyc A, Jankauskiene A, Ekim M, Edefonti A, Bakkaloğlu SA. **The effects of hospital and dialysis unit characteristics on hospitalizations for access-related complications among children on maintenance dialysis: a European, multicenter, observational, cross-sectional study. Pediatr Nephrol.** 2023 Jul;38(7):2189-2198. doi: 10.1007/s00467-022-05842-5. Epub 2023 Jan 3. PMID: 36595069.
7) Veres-Székely, Apor; Szebeni, Beáta; Pap, Domonkos; Bokrossy, Péter; **Lévai, Eszter**; Szász, Csenge; Szabó, J. Attila; Vannay, Ádám - **A fibroblastok funkcionális vizsgálata – IV. rész: Az ECM-termelés mérése („The functional examinations of fibroblasts – Part IV. – Measuring ECM production"), Gyermekgyógyászat 2022;** 73. évfolyam, 6. szám (2022)
8) Veres-Székely A, Pap D, Szebeni B, Őrfi L, Szász C, Pajtók C, **Lévai E**, Szabó AJ, Vannay Á. **Transient Agarose Spot (TAS) Assay: A New Method to Investigate Cell Migration. Int J Mol Sci. 2022** Feb 14;23(4):2119. doi: 10.3390/ijms23042119. PMID: 35216230; PMCID: PMC8880674.
9) Atikel YÖ, Bakkaloğlu SA, Paglialonga F, Stefanidis CJ, Askiti V, Vidal E, Ariceta G, Melek E, Verrina E, Printza N, Vondrak K, Zurowska A, Zagozdzon I, Ekim M, Özmert EN, Dufek S, Jankauskiene A, Schmitt CP, **Levai E,** Walle JV, Canpolat N, Holtta T, Fischbach M, Zaloszyc A, Klaus G, Aufricht C, Shroff R, Edefonti A. **Influenza and pneumococcus vaccination rates in pediatric dialysis patients in Europe: recommendations vs reality A European Pediatric Dialysis Working Group and European Society for Pediatric Nephrology Dialysis Working Group study. Turk J**

Med Sci. 2021 Dec 13;51(6):2881-2886. doi: 10.3906/sag-2012-26. PMID: 33535736; PMCID: PMC10734874.

10) Bakkaloğlu SA, Özdemir Atikel Y, Paglialonga F, Stefanidis CJ, Askiti V, Vidal E, Ariceta G, Melek E, Verrina E, Printza N, Vondrak K, Zurowska A, Zagozdzon I, Ekim M, Özmert EN, Dufek S, Jankauskiene A, Schmitt CP, **Lévai E**, Vande Walle J, Canpolat N, Holtta T, Fischbach M, Klaus G, Aufricht C, Shroff R, Edefonti A. **Vaccination Practices in Pediatric Dialysis Patients Across Europe. A European Pediatric Dialysis Working Group and European Society for Pediatric Nephrology Dialysis Working Group Study. Nephron. 2018;**138(4):280-286. doi: 10.1159/000485398. Epub 2017 Dec 12. PMID: 29232664.

11) **Lévai, E**., Pethő-Orosz, P., Kelen, K., Mészáros, K., Sallay, P., Reusz, G., Magdás, A., & Szabó, A. (2017**). Peritonealis dialízis gyermekkorban. A Semmelweis Egyetem I. Gyermekgyógyászati Klinikájának eredményei. Orvosi Hetilap** OH, 158(46), 1831-1840. https://doi.org/10.1556/650.2017.30857

10 Acknowledgements

First of all, I would like to thank my mentors, Prof. Claus Schmitt and Prof. Attila Szabó, without whom I could have never improved this much over the years, discover so interesting questions (sometimes even answers) and fields, and who always inspired me to do more and better and still continue to do so. They both gave me so many opportunities, invaluable professional and life-advice and it would be another 50 pages to get into detail how I was helped on my road, them letting me do it my way. I am incredibly grateful for that!

My absolutely cherished time in Heidelberg was a) a perfect decision, b) I am grateful for all the things I have learned from and experienced together with Maria Bartosova from the start and then on all and everything that can't even be described that I got from Iva and Conghui, who all became my role models and close-close friends. Theresa, my dearest Mint, Jana and Tillmann, I am happy I had and have you in my life, and thanks to Shabnam, Barbara and Bärbel for helping me so much.

I have to thank Betti, Akos, Sotiris (my scientific Godfather), Christina and Evangelina and Akoska (for sure two shining stars of the future) for including me in their second family. Those were golden times, and I can't put it into words, but you know how much it means to me, for sure.

Thanks to Csenge for maintaining my sanity in all situations, and who I was the luckiest to sit next to for some of the most treasured times in my life. To my group of friends from the Budapest Lab, especially Tamás and Ákos for their support, full-blown insanity, laugh and joy and having that feeling of family at work, which is much needed starting a PhD.

My ride-or-dies, continuously connecting me to all other aspects of life - Dóra and Dóri, Vivi, Máté, Tomi, Ambrus and Pitás and my oldest, dearest friends Eszti, Réka, and Zsófi and many others who made sure I am not lost in the process, because no matter how much I loved most of it, I still could have been. Thanks to Nándi for contributing to a more balanced everyday life, and finish of this work, and to be also continuously curious with me about everything.

I want to thank my colleagues from the Research Lab of the Pediatric Center in Budapest, especially Apor, Marcsi and Doma, for teaching me a lot restlessly and having fun in the

meantime, and all the members of the Vannay Lab from whom I have learnt a lot about scientific thinking and rigor.

Thanks to my colleagues and friends in the clinic, especially Kriszta, Dia and Vera, and doctor and nurse colleagues from the Nephrology and Dialysis Department whom I can learn so much from, and who were gracious to welcome me in their lively and motivated community and of course our patients and their families both in Heidelberg and Budapest.

I am grateful for the support of the Kerpel-Fronius Ödön Talent Programme of Semmelweis University, the Jellinek-Harry Scholarship and EJP-RD Research Mobility Program, which made possible for me to spend so much time in Heidelberg, and ERKNET and ESCAPE and Prof. Franz Schaefer for letting me learn in the close-knit circle of European pediatric nephrology.

Last, but not least, I would like to thank my parents and my uncle, because they gave me the world with the mindset I was raised with (and also literally) and were and are great examples of staying curious and working hard, doing it with grace and love for the field they explore, and of course a really great sense of humor. They have supported me through all, and they do deserve at least half a degree for this PhD too. (That is a lot of degrees.)

And as it is getting cloudy, this chapter both literally and figuratively speaking needs to end for another one to start. Thank you!

Own work

In this dissertation I insist on the usage of the plural form, because I strongly believe that advances in life sciences nowadays always require a group effort, and throughout the years of my PhD studies I was lucky enough to work with and be formed by a fantastic group of individuals. Because of that and out of respect of our unity as a group, I intended to use "we" forms and also because I wanted to show an overarching idea about the molecular counterparts and function of the peritoneal membrane, made out of multiple puzzle pieces, worked and discussed throughout the process of these investigations by many.

Of course, as it is a PhD-dissertation with the goal of assessing my added value to the chosen field of science, I would like to specify my own work in these projects.

1. Description of tight junction proteins in the peritoneal membrane in health, CKD and during PD:

   -I partly conceptualized the study, performed most of the quantitative immunohistochemistry (IHC) experiments for CLDN1-5, ZO-1 and OCL, and to a smaller extent to TriC, CLDN15, PiT1, SGLT1 and ENaC. I did the quantitative analysis of the IHC and analyzed the clinical data of our patients and partly did the statistical analysis of functional data and abundance data of our investigated molecules. We interpreted our data together with my shared first co-author on the associated paper, Dr. Marinovic.
2. Establishing an experimental workflow for studying barrier integrity, permeability and TJ composition and localization in a single endothelial cell monolayer

   -I performed in vitro experiments, to measure TER and fluorescent labeled dextrane flux in Transwell systems and completed part of the immunofluorescent stainings for imaging, also performed experiments to establish the right protocol for SMLM microscopy staining on Transwell filters. I also analyzed data from the Transwell experiments.
3. Investigation of AlaGln as an additive to improve endothelial barrier function

- I performed in vitro Transwell experiments measuring TER and fluorescent labeled dextrane flux and analyzed data. Performed protein quantification of CLDN5 and ZO-1 by Western Blots and analyzed data.

4. Studying GDP induced vasculopathy in children on chronic peritoneal dialysis

   -I performed in vitro experiments on Transwells with 3,4-DGE treatment and measured TER and fluorescent-labeled dextrane flux. Performed immunofluorescent stainings and Western Blot protein quantification. Before helped to establish the right protocol for cell monolayers and tissues for SMLM microscopy.

At every other result displayed for helping the deeper understanding of the work, I refer to the performing scientist properly and they have agreed to the presentation of our common data.